Damage Tolerance and Durability of Fiber-Metal Laminates for Aircraft Structures

Professor Jenn-Ming Yang

The Joint Advanced Materials and Structures Center of Excellence

FAA Sponsored Project Information

- **Principal Investigators & Researchers**

Hyoungseock Seo, PhD candidate
Po-Yu Chang, PhD candidate
Professor H. Thomas Hahn
Professor Jenn-Ming Yang
Department of Mechanical & Aerospace Engineering
Department Materials Science Engineering
University of California, Los Angeles

- **FAA Technical Monitor**
  - **Mr. Curtis Davies**
- **Other FAA Personnel Involved**
  -
- **Industry Participation**
  -Raytheon Missile Systems

Damage Tolerance and Durability of Fiber-Metal Laminates for Aircraft Structures

- ## Motivation and Key Issues
  - Fiber metal laminate is a new generation of primary structure for pressurized transport fuselage. However, there are limited and insufficient information available about mechanical behavior of FML in the published literature, and some areas still remains to be further verified by more detailed testing and analysis.
- ## Objective
  - To investigate the damage tolerance and durability of bi-directionally reinforced GLARE laminates. Such information will be used to support the airworthiness certification and property optimization of GLARE structures
- ## Approach
  - To develop analytical methods validated by experiments
  - To develop information system

Background

- **GLARE (S2-glass fiber reinforced Al) laminates**
  - Hybrid composites consisting of alternating thin metal layers and glass fibers
- **Advantages of GLARE**
  - High specific properties and low density
  - Outstanding fatigue resistance
  - Excellent impact resistance and damage tolerance
  - Good corrosion and durability
  - Easy inspection like aluminum structures
  - Excellent flame resistance

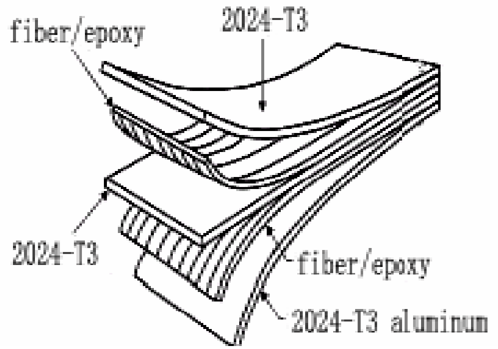

Project Scope

To develop methodologies for guiding material development, property optimization and airworthiness certification:

- **Residual Strength Modeling and Validation**
  --open-hole notch strength
  --residual strength after impact
  --open-hole notch strength after fatigue
- **Impact and Post-Impact Fatigue Behavior**
- **Numerical Simulation of single and Multiple Impact**
- **Fatigue Crack Initiation/Growth Modeling and Validation**
  --constant amplitude fatigue
  --variable amplitude fatigue
- **Multi-site Fatigue Damage**
- **Information System for Certification**

Multi-Site Fatigue Damage

- Multi-site fatigue damage occurred in in-service airliner fuselage, for instance, Aloha airline accident in 1988.

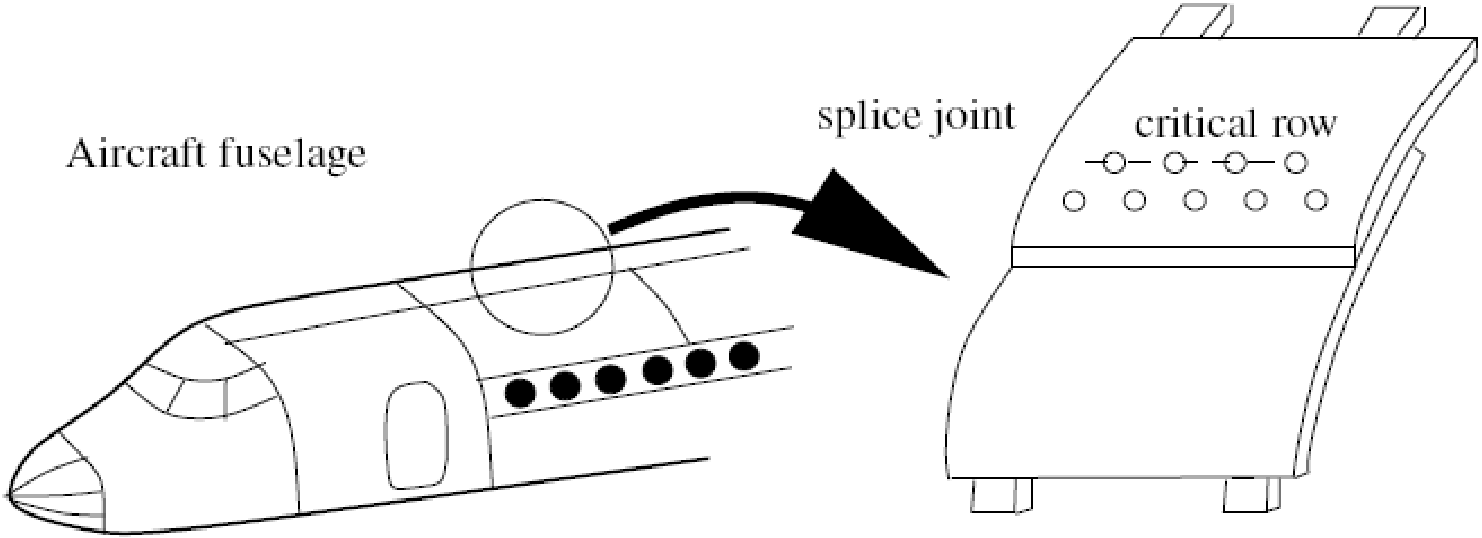

Crack link-up of in-service aluminum fuselage with multiple-site damage (MSD)

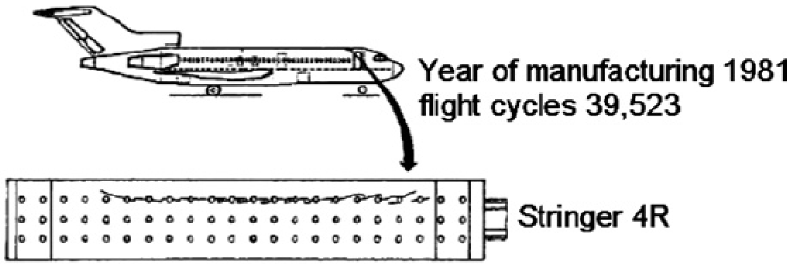

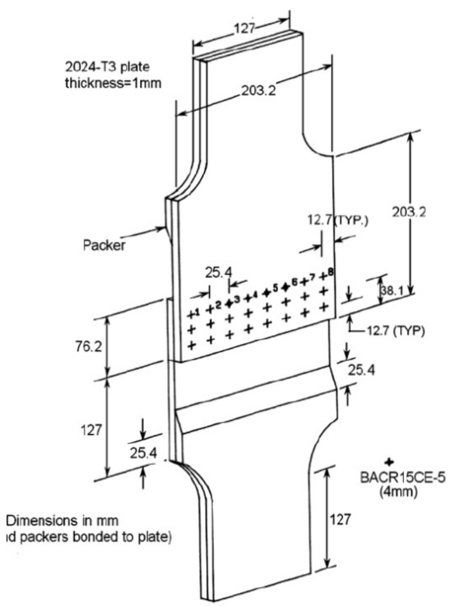

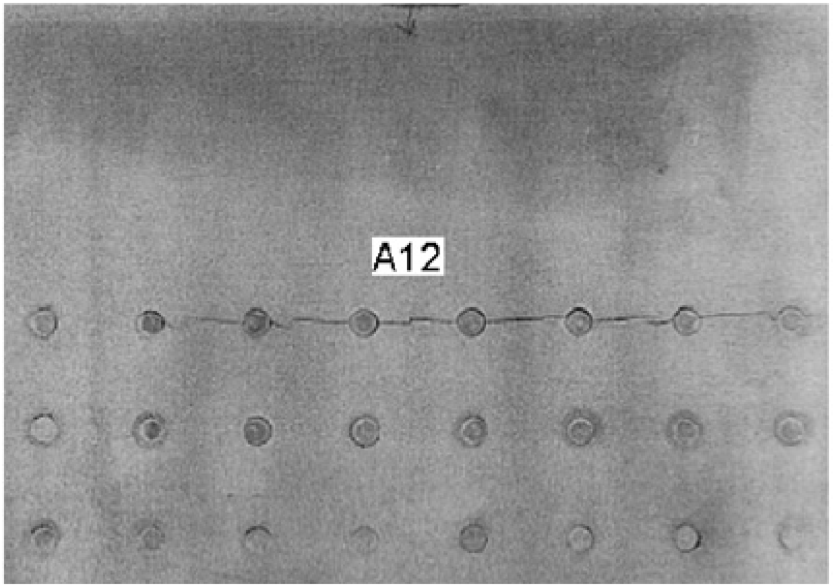

Jones, R; Molent, L; Pitt, S, Understanding crack growth in fuselage lap joint, Theoretical and applied fracture mechanics 2008 v49,n1, p38--50

On-going crack Interaction

- Crack tips link-up at plastic zones with the presence of multiple-site damage.

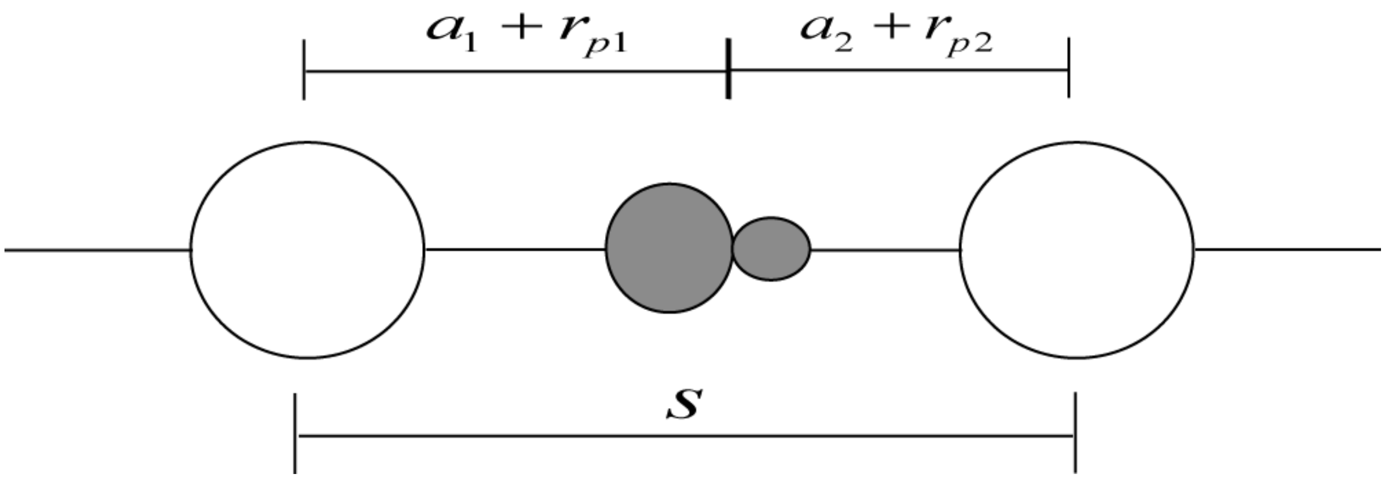

Crack growth in aluminum with MSD

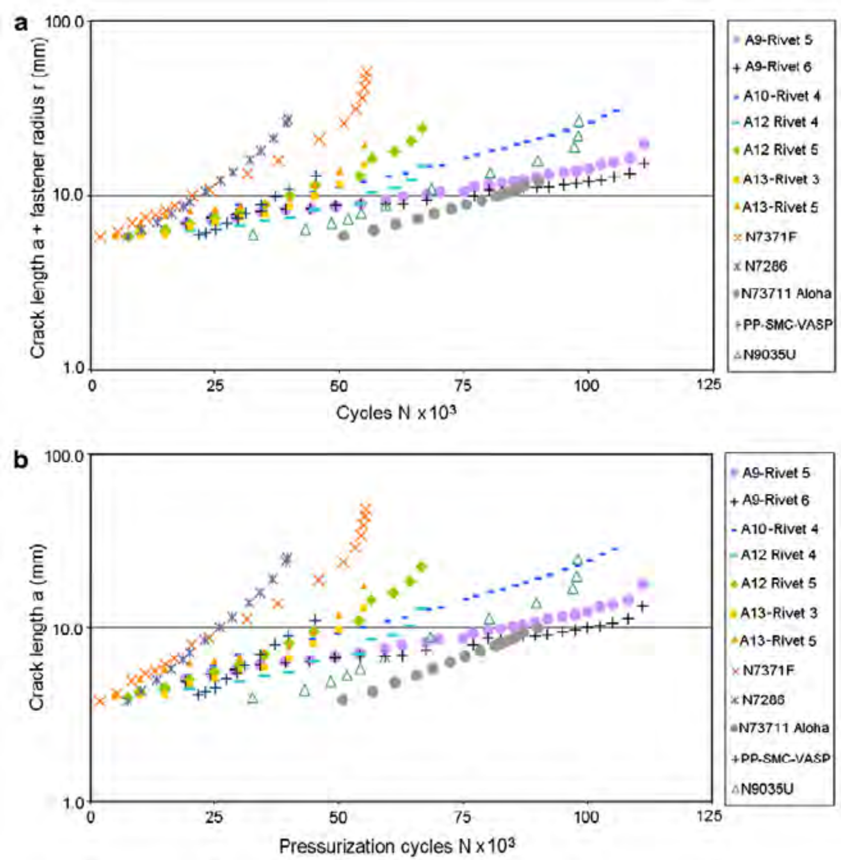

Jones, R; Molent, L; Pitt, S, Understanding crack growth in fuselage lap joint, Theoretical and applied fracture mechanics 2008 v49,n1, p38--50

Crack growth in fiber metal laminates

- Left: bridging mechanism in FML.
- Right: fatigue life of monolithic Al alloy and GLARE laminates.

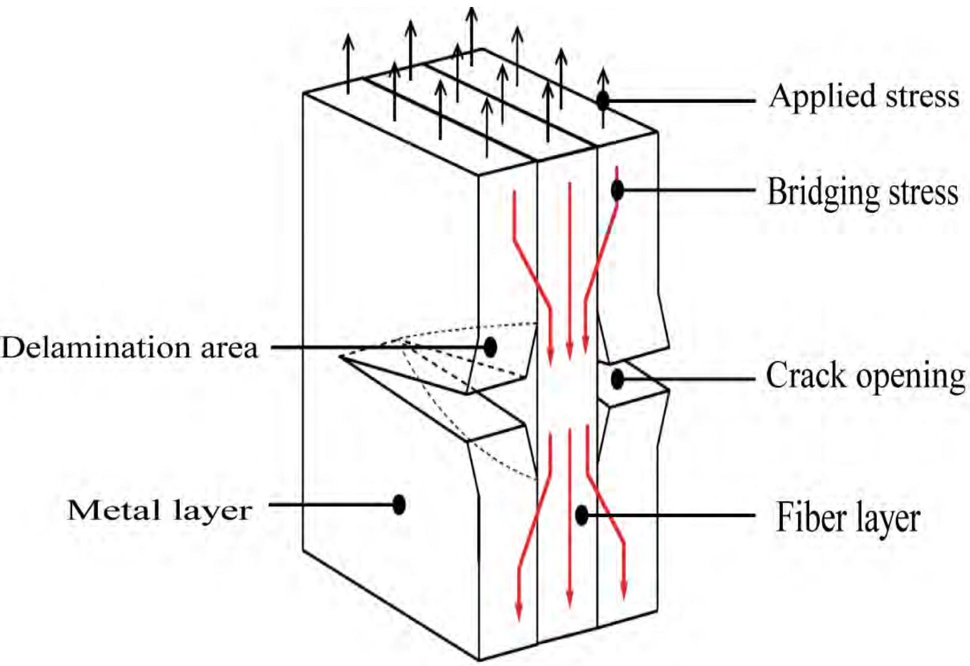

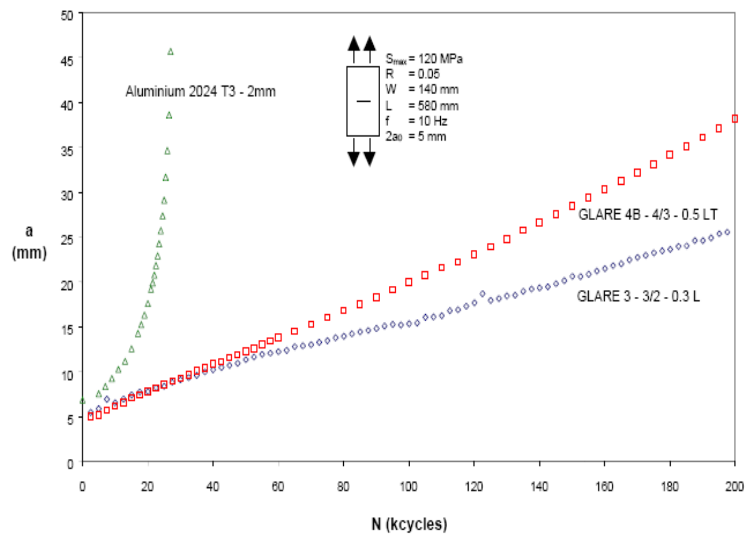

Vlot A, Gunnink JW, editors. Fibre metal laminates—an introduction. Kluwer Academic Publishers; 2001.

Delamination front-fiber/adhesive

- Delamination link-up at front with the presence of multiple-site fatigue damage.
- Materials: Glare3-3/2

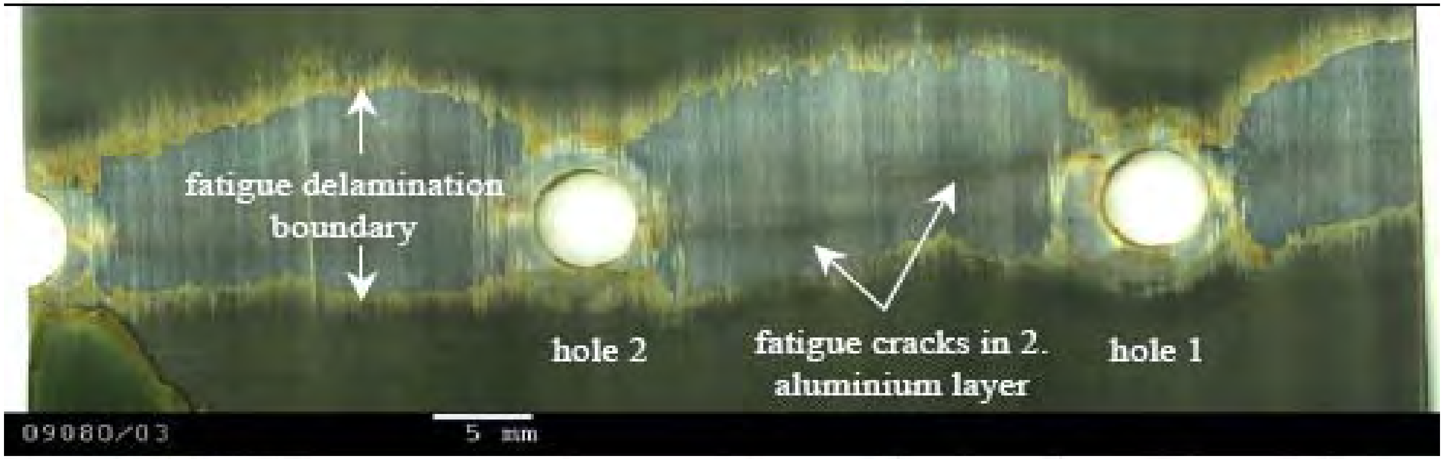

Configuration of specimens with MSD

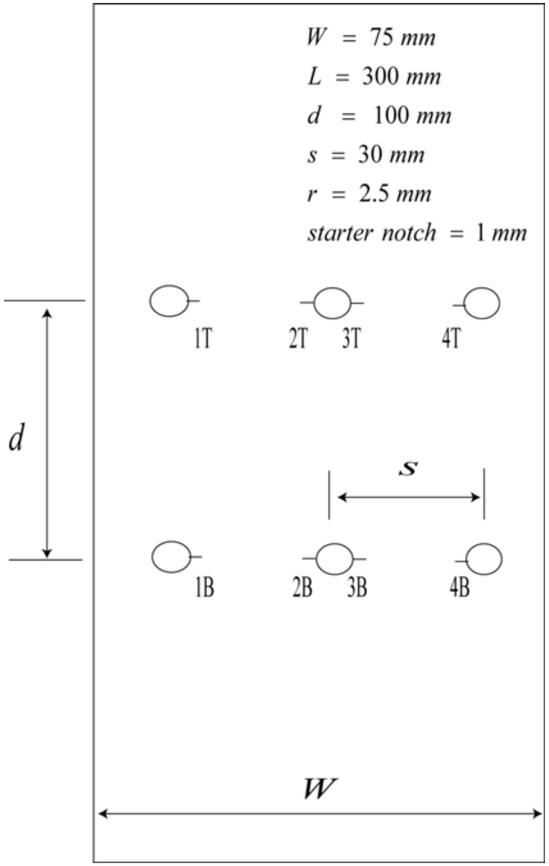

Surface crack propagation

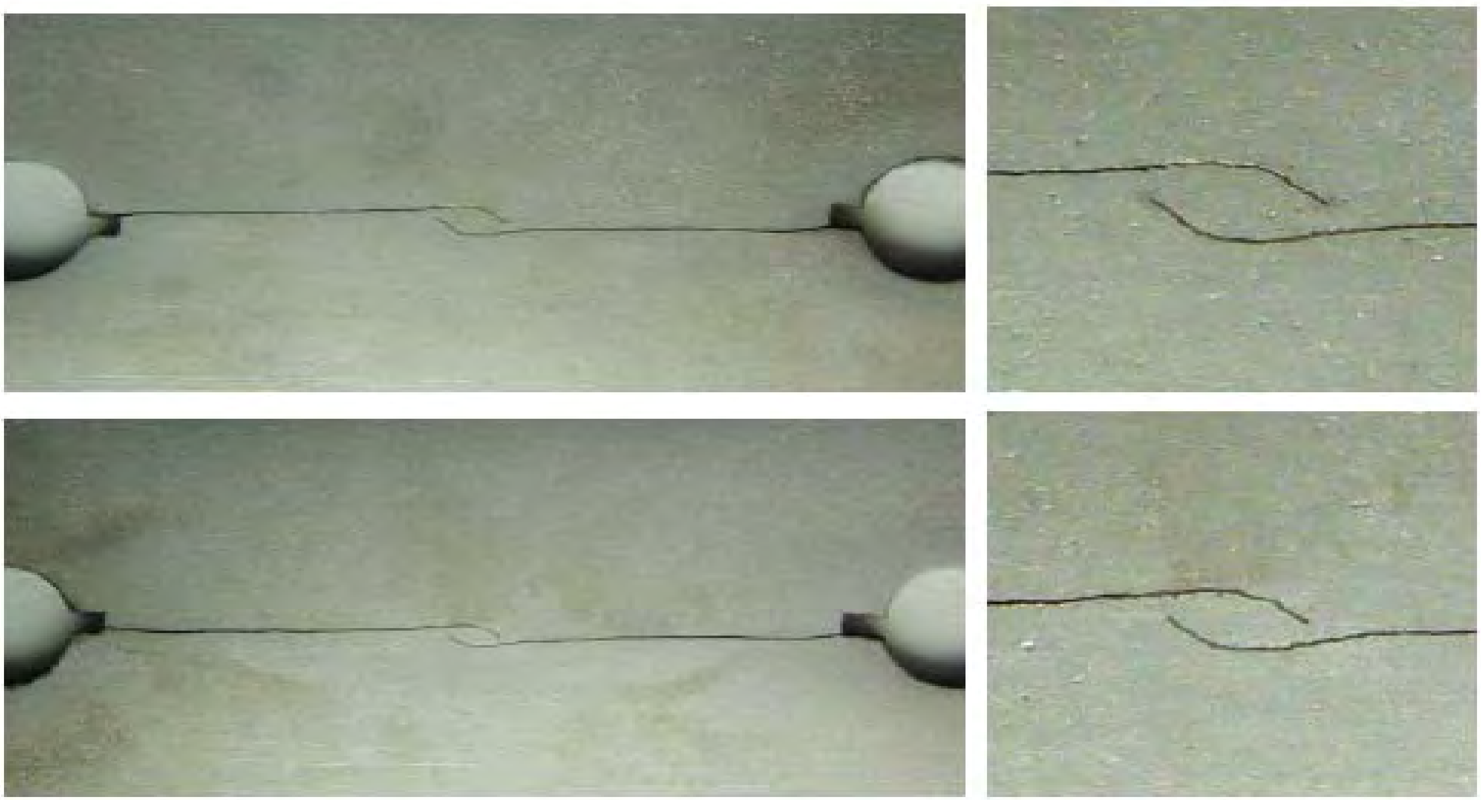

Crack growth in surface and inner metal layer

- Top: surface metal layer
- Bottom: inner metal layer

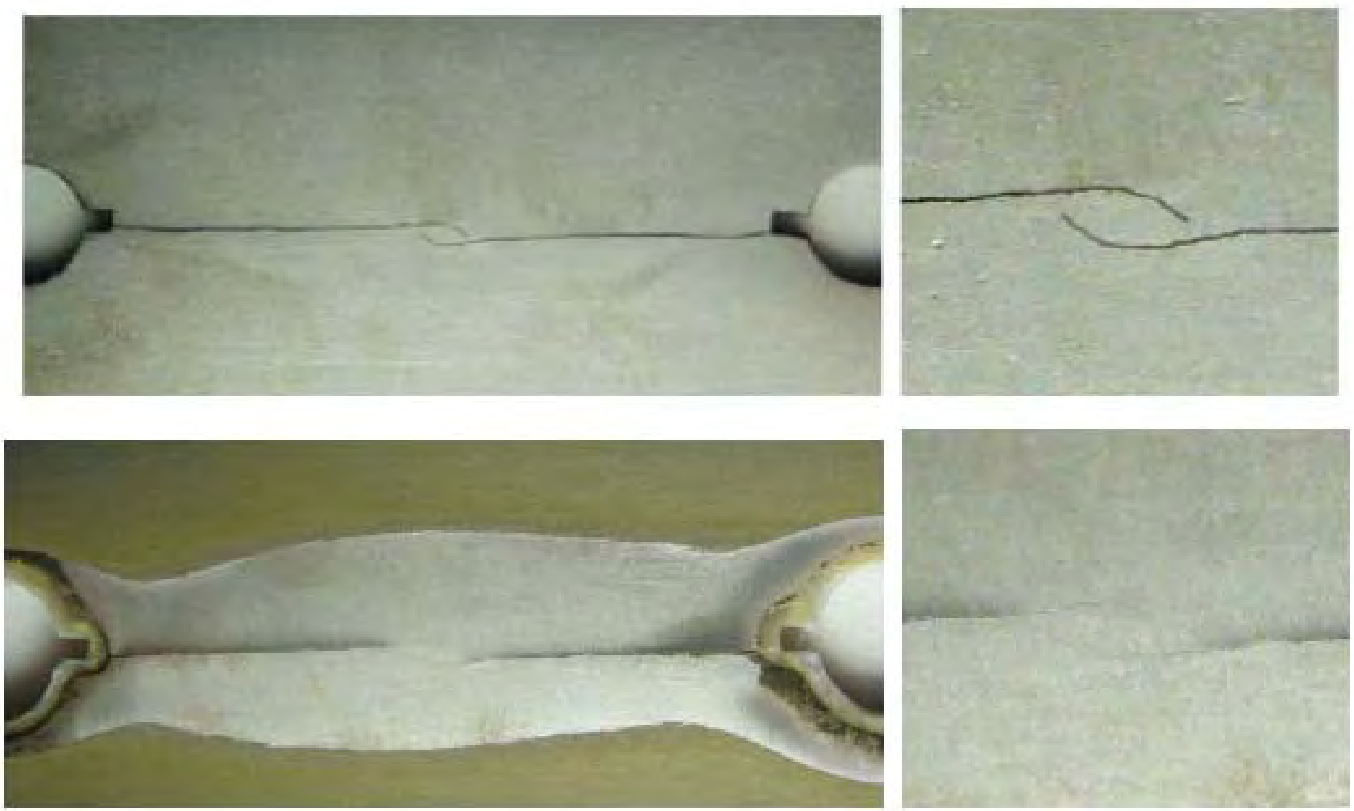

MSD delamination growth

- Left: delamination propagation
- Right: delamination link-up

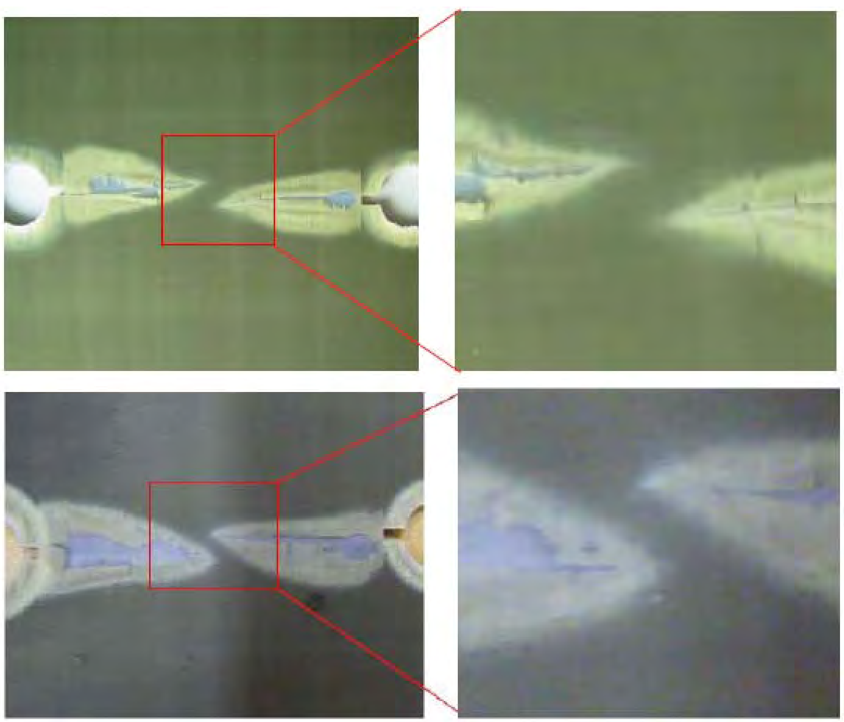

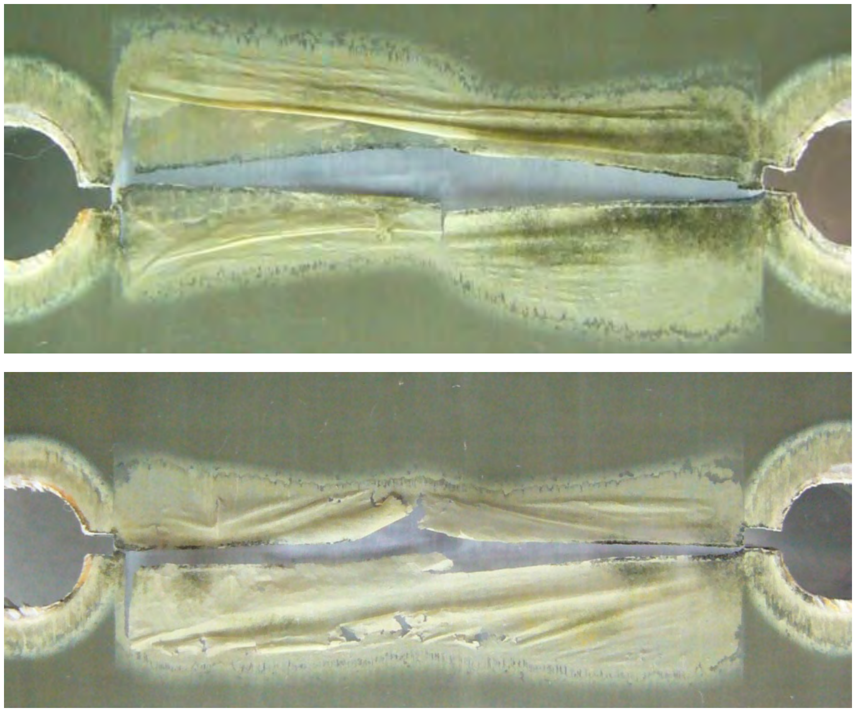

Top-row crack growth

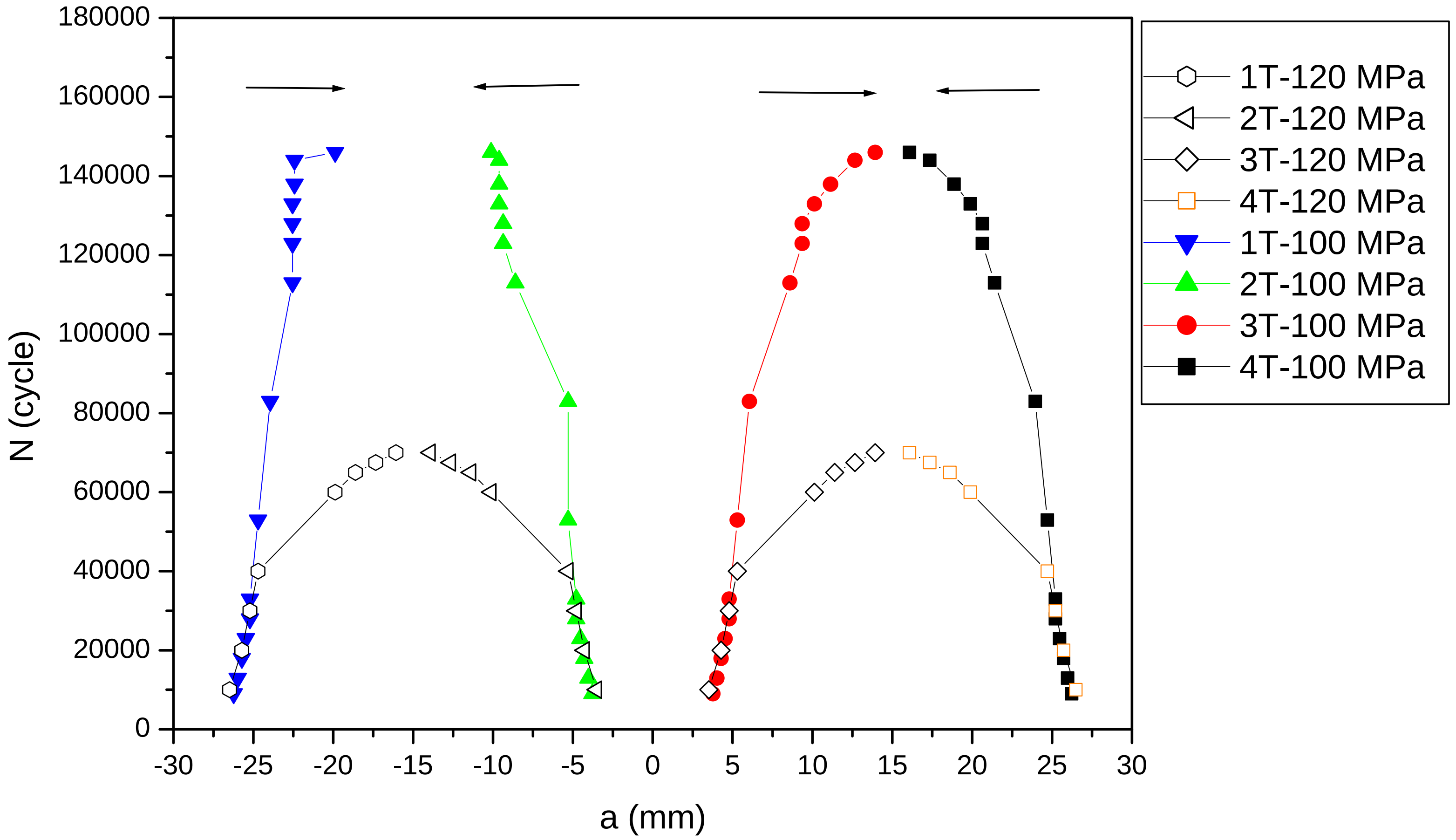

Bottom row crack growth

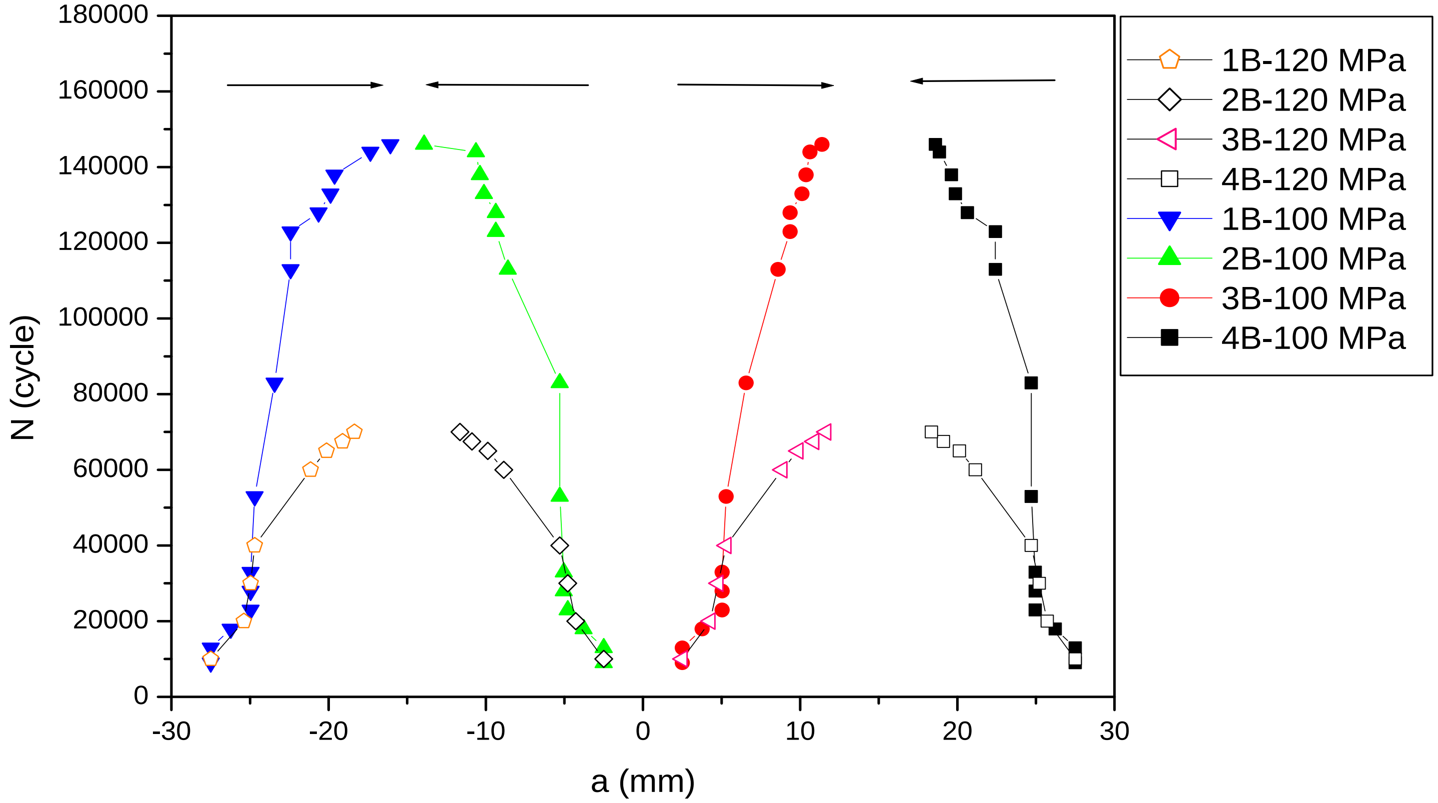

Experimental crack growth rates

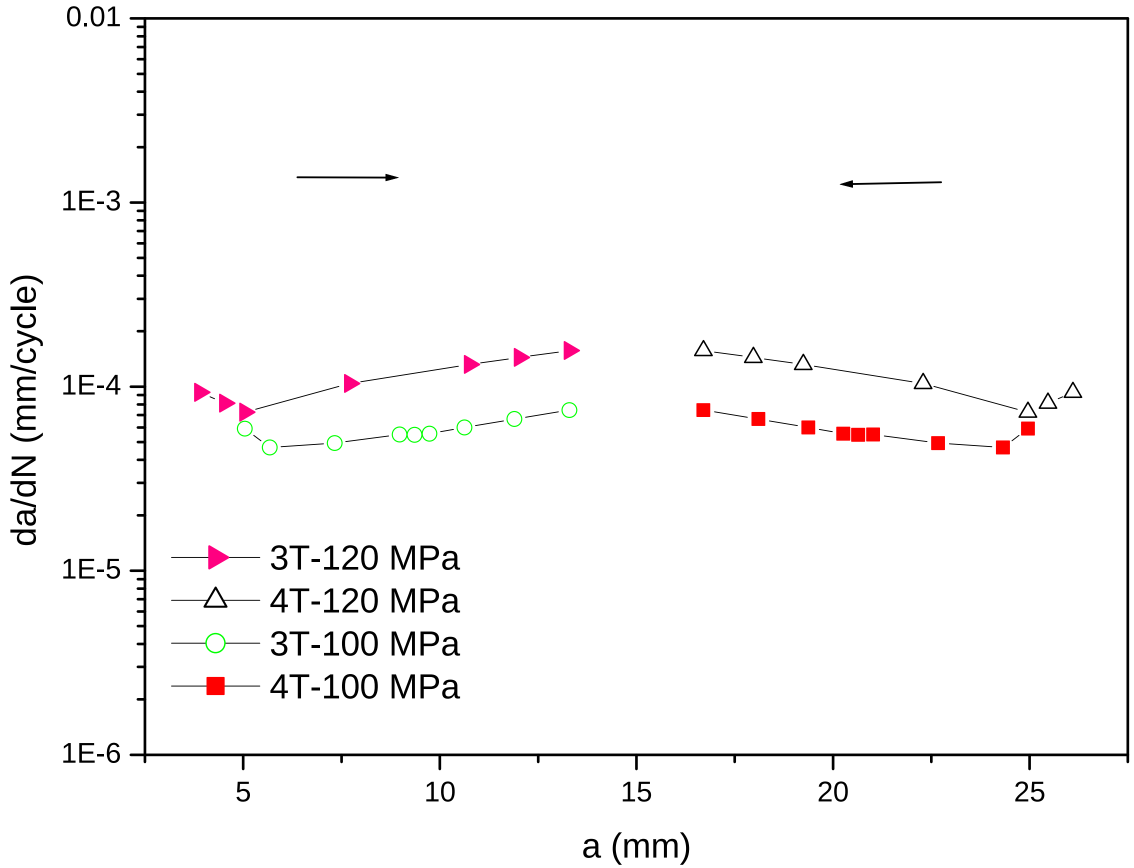

Prediction model of crack growth

- Define effective stress intensity factor with bridging factor.
- Empirical Paris fatigue law is used from monolithic Al alloy.

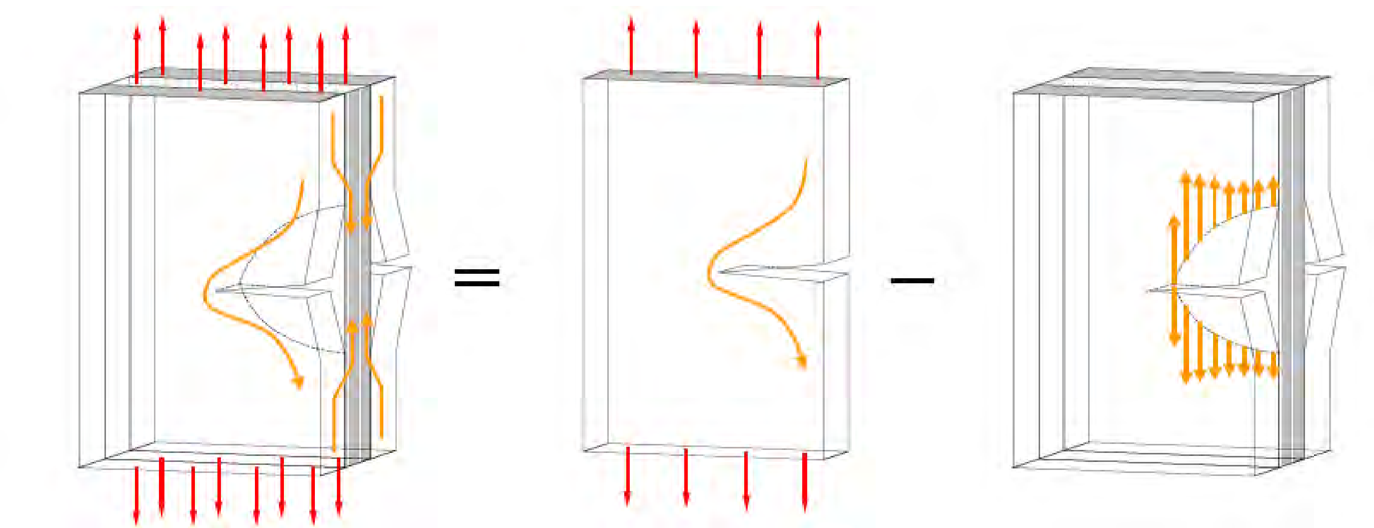

$$\frac{da}{dN} = C_g \left(\Delta K_{eff} \right)^{n_g}$$

$$K_{eff} = (K_{re} - K_{op})(1 - \beta), \ \beta = K_{br} / K_{re}$$

Stress analysis with no multiple-site fatigue damage

- Actual stress level in metal layer is higher than the applied stress.

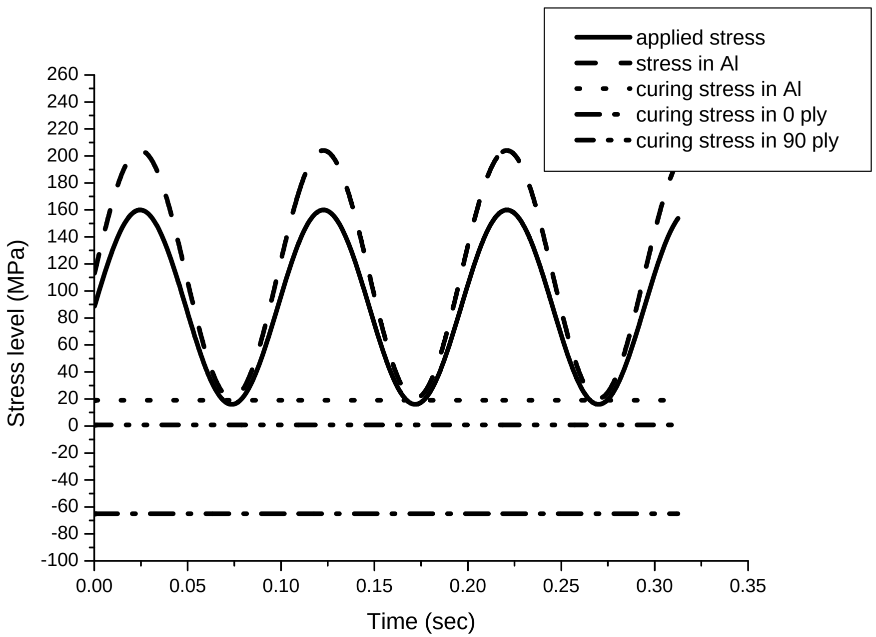

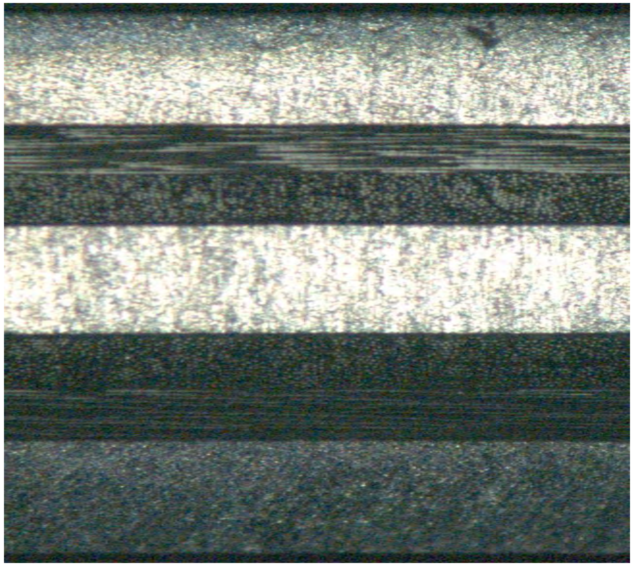

Po-Yu Chang, Jenn-Ming Yang, et al. (2007) Off-axis fatigue cracking behavior of notched fiber metal laminates. Fatigue Fract Eng Mater Struct.30:158-1171.

Stress analysis with multiple-site fatigue damage

- Stress concentration around notched holes.

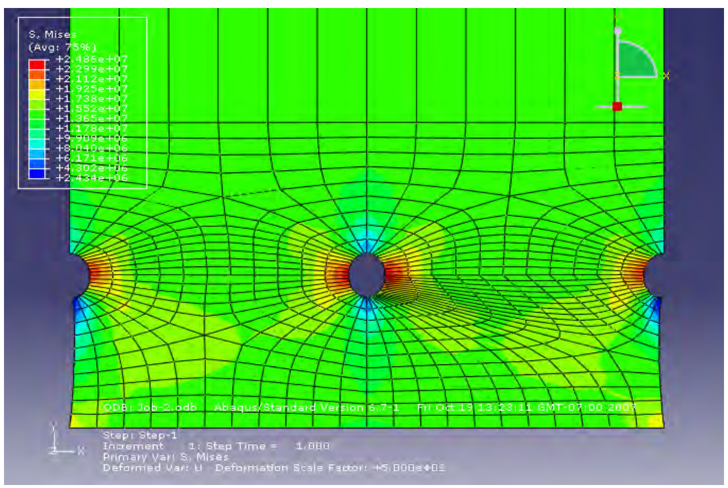

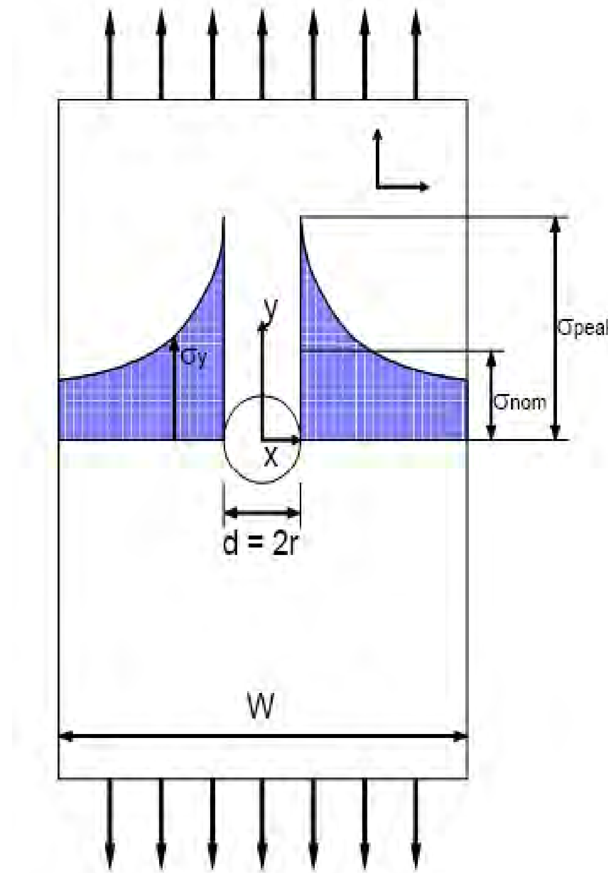

Far-field stress intensity factor

- Stress intensity factor for interaction and non-interaction cracks

$$K_A = \left[\sigma\left(\pi a_1\right)^{1/2} f_{2h}\right] f_A f_w$$

$$K_B = \left[\sigma\left(\pi a_2\right)^{1/2} f_h\right] f_B f_l$$

$$K_C = \left[\sigma\left(\pi a_3\right)^{1/2} f_{2h}\right] f_A f_w$$

Schijve, International Journal of Fatigue, 1993

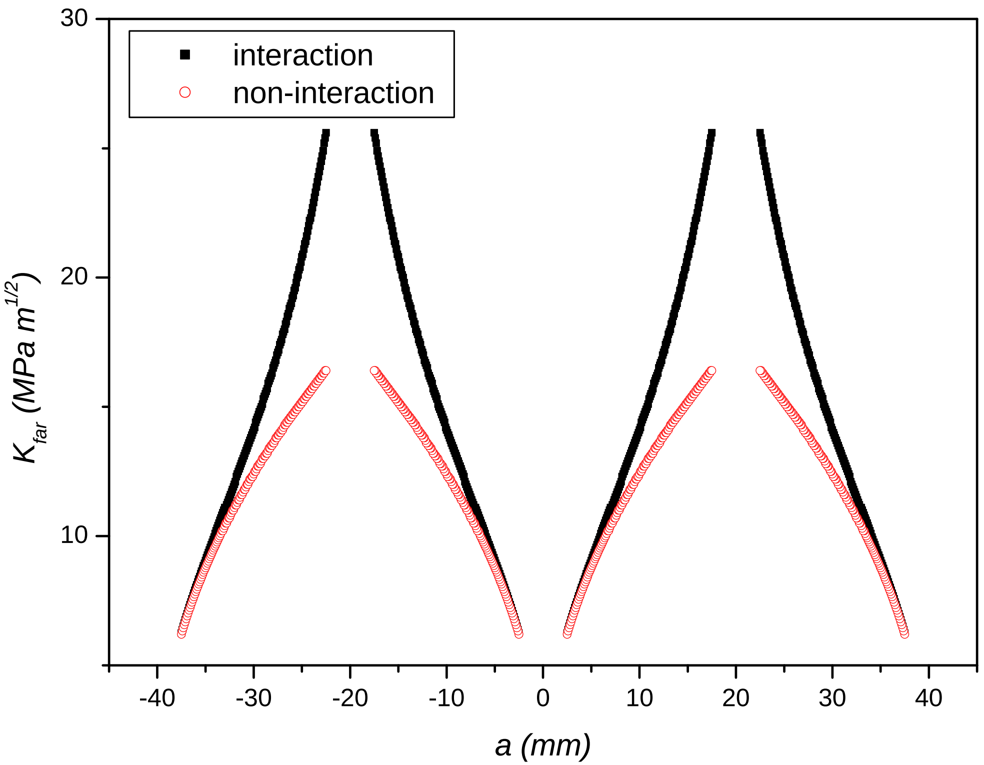

Crack opening relations

- Crack opening induced by the applied load – crack closing restrained by the bridging stress = deformation in fiber elongation + deformation in prepreg + deformation in metal layer.

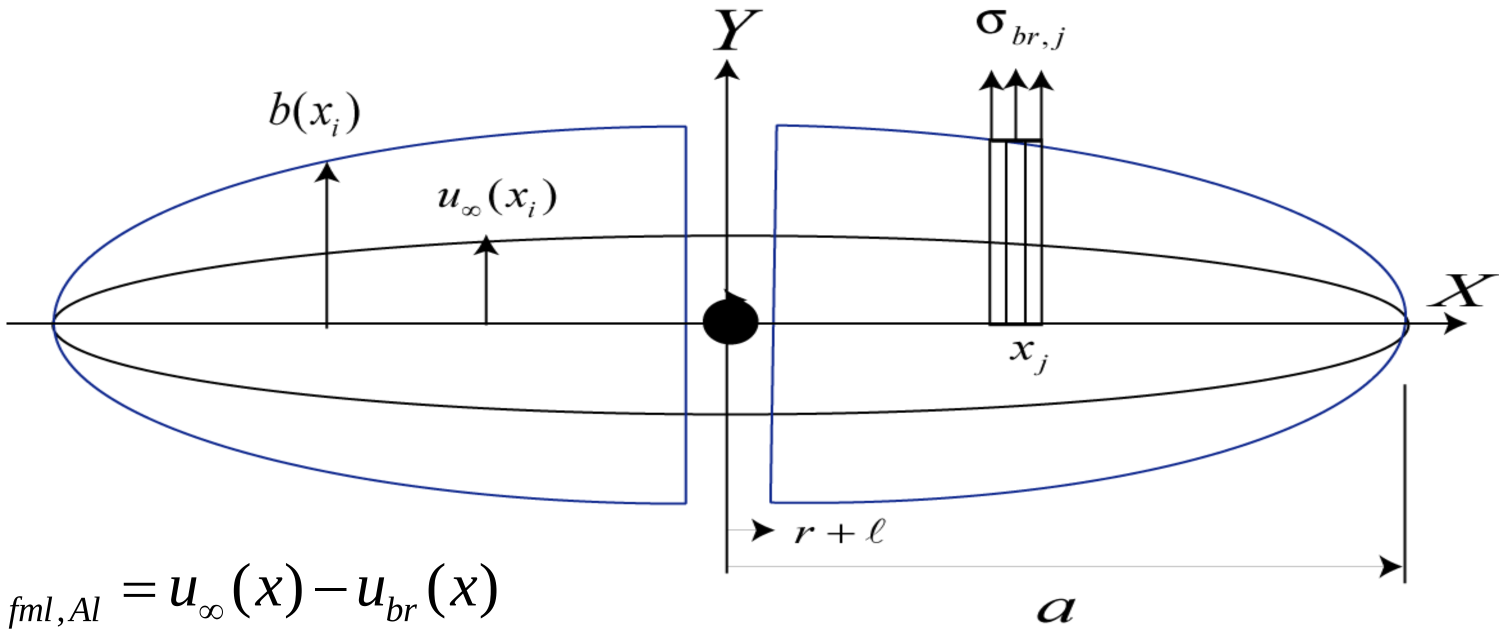

$$u_{fml,Al} = u_\infty(x) - u_{br}(x)$$

$$u_{fml,Al} = \delta_f(x) + \delta_{pp}(x) + \delta_{Al}$$

Guo YJ, Wu XR. (1999) Bridging stress distribution in center-cracked fiber reinforced metal laminates: modelling and experiment. Eng Fract Mech; 63:147–63.

Calculation of bridging stress

- Governing equation

$$\sigma_{br} = M_j^{-1} N$$

$$N = u_\infty(x) - \delta_{pp}(x) - \frac{\sigma_f}{E_f} b(x)$$

$$M_j = \sum \frac{u_{br}(x_i, x_j)\Delta x_j}{\sigma_{br}(x_j)} - \frac{b(x_i)}{E_f}\delta(i, j)$$

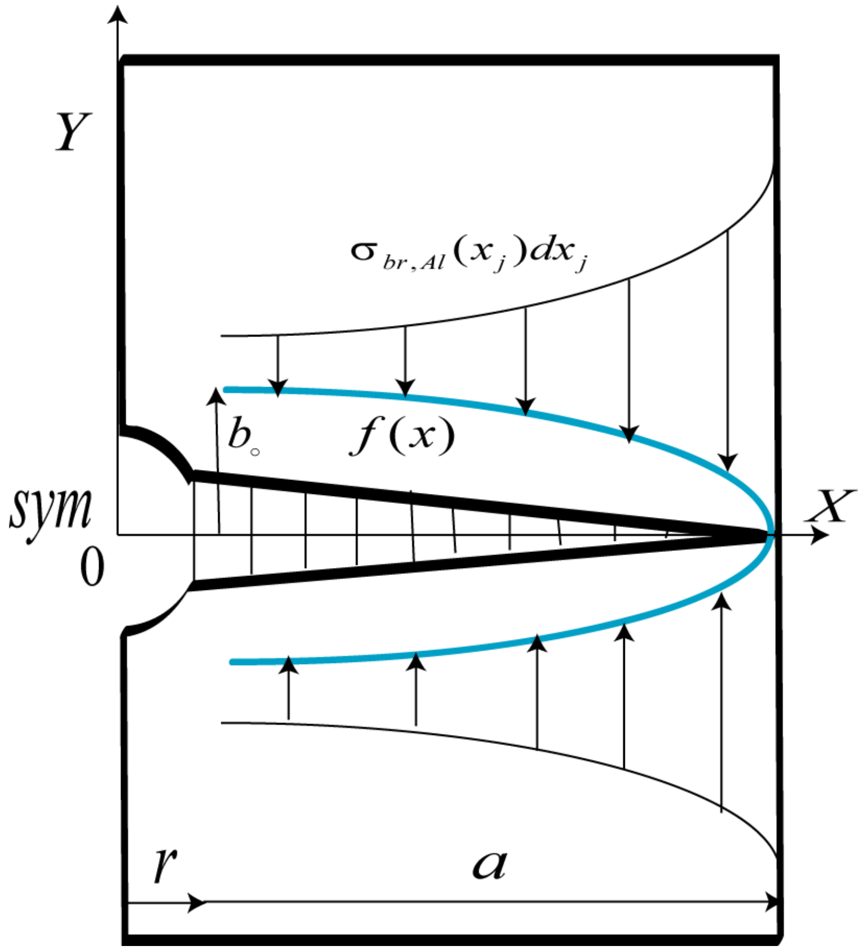

Bridging stress distribution

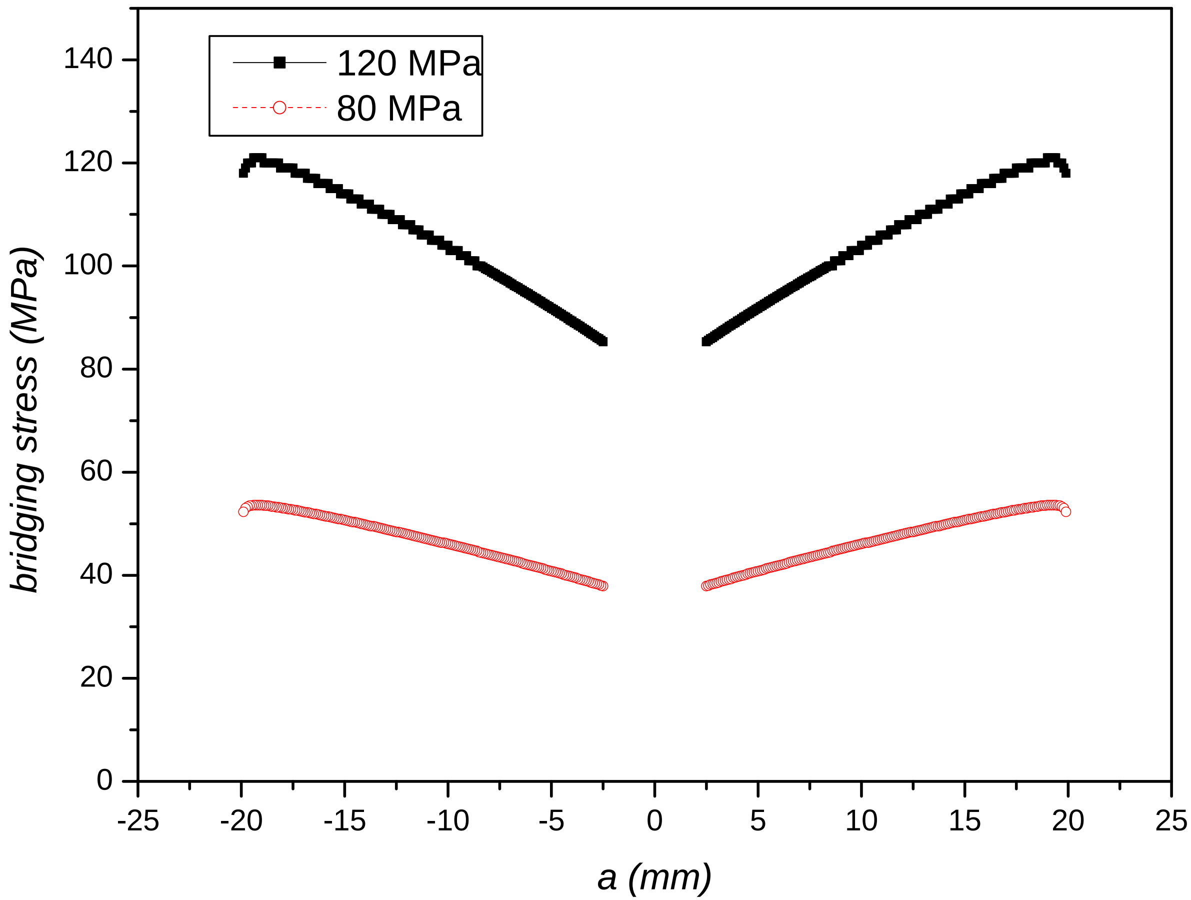

Bridging stress intensity factor

- Concept: energy balance based on virtual work
- Equivalent bridging stress on the crack flanks.

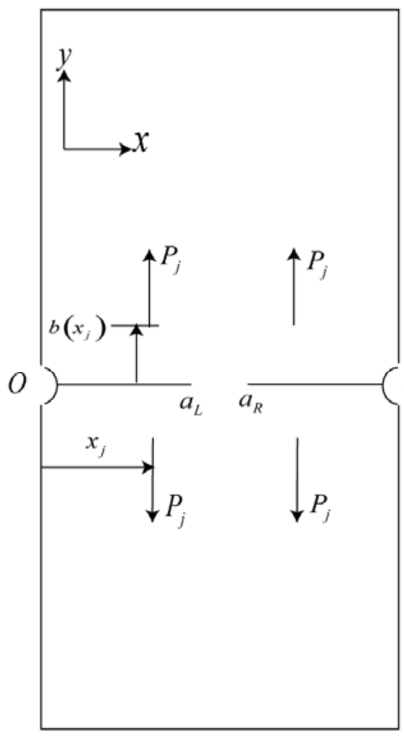

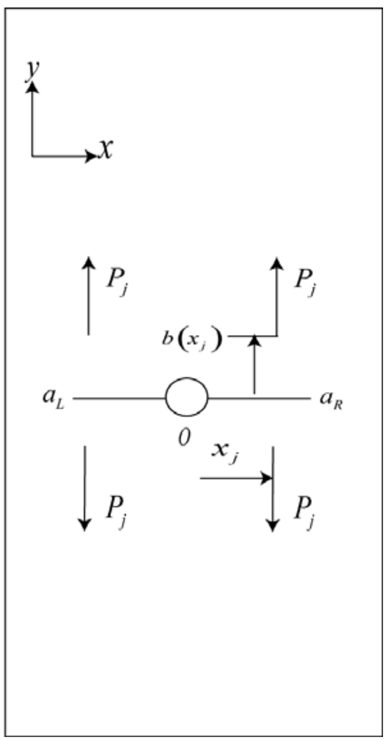

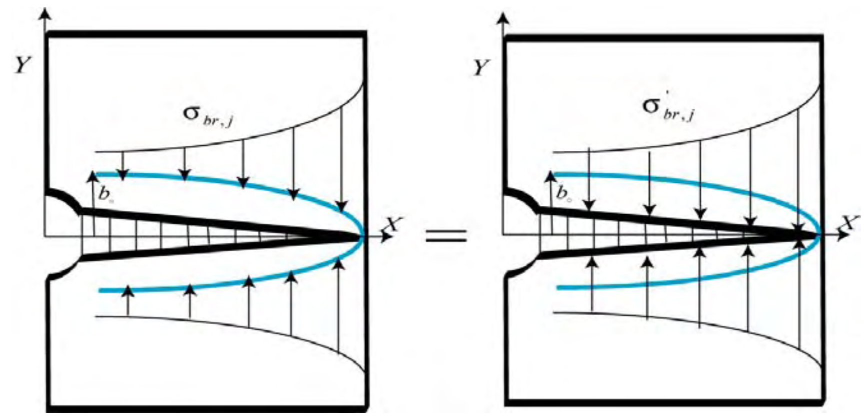

$$K_{br,j} = \sum_{j=i}^{N} \frac{2\sigma'_{br,Al,j}\Delta x_j}{\sqrt{\pi s}} \frac{\sqrt{\tan(\frac{\pi a}{s})\cos(\frac{\pi x_j}{s})}}{\sqrt{(\sin\frac{\pi a}{s})^2-(\sin\frac{\pi x_j}{s})^2}}$$

Bridging factors

- The dimensionless bridging factors flat out after an initial sharp rise.
- This transition implies crack growth of FMLs reaching approximately steady state.

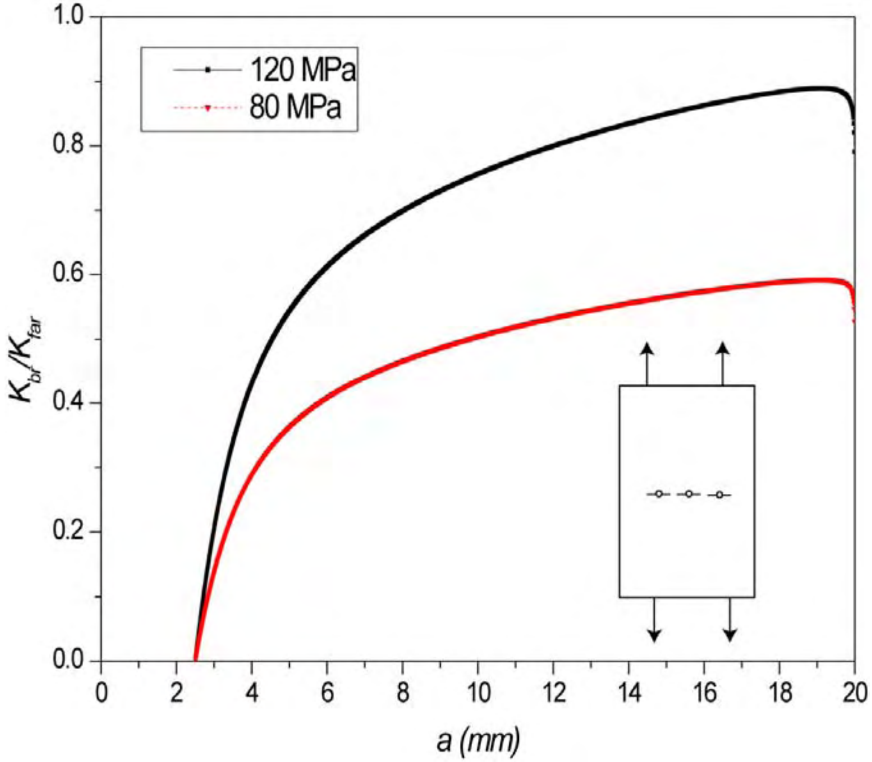

Effective stress intensity factor

- Effective stress intensity factor reaches approximately constant. (steady state crack growth)

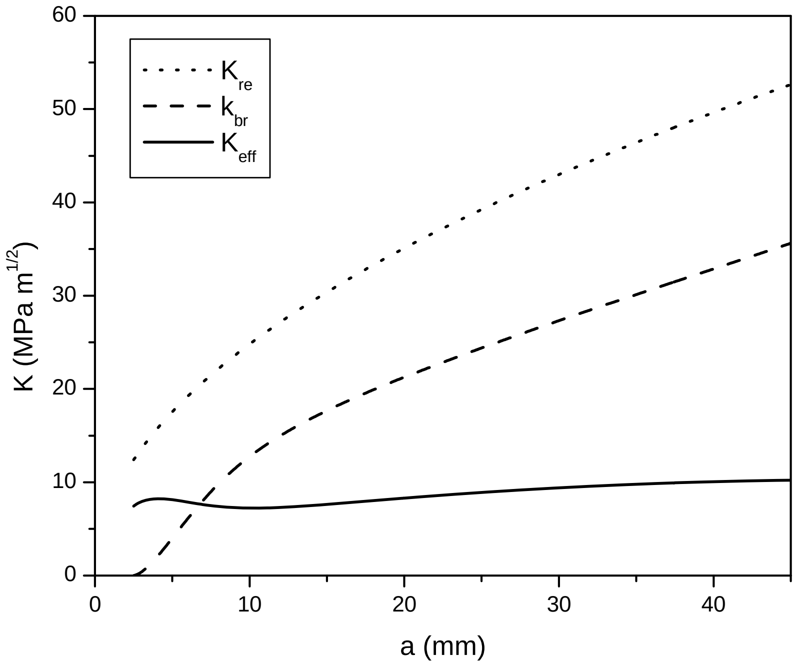

Experimental crack growth rates

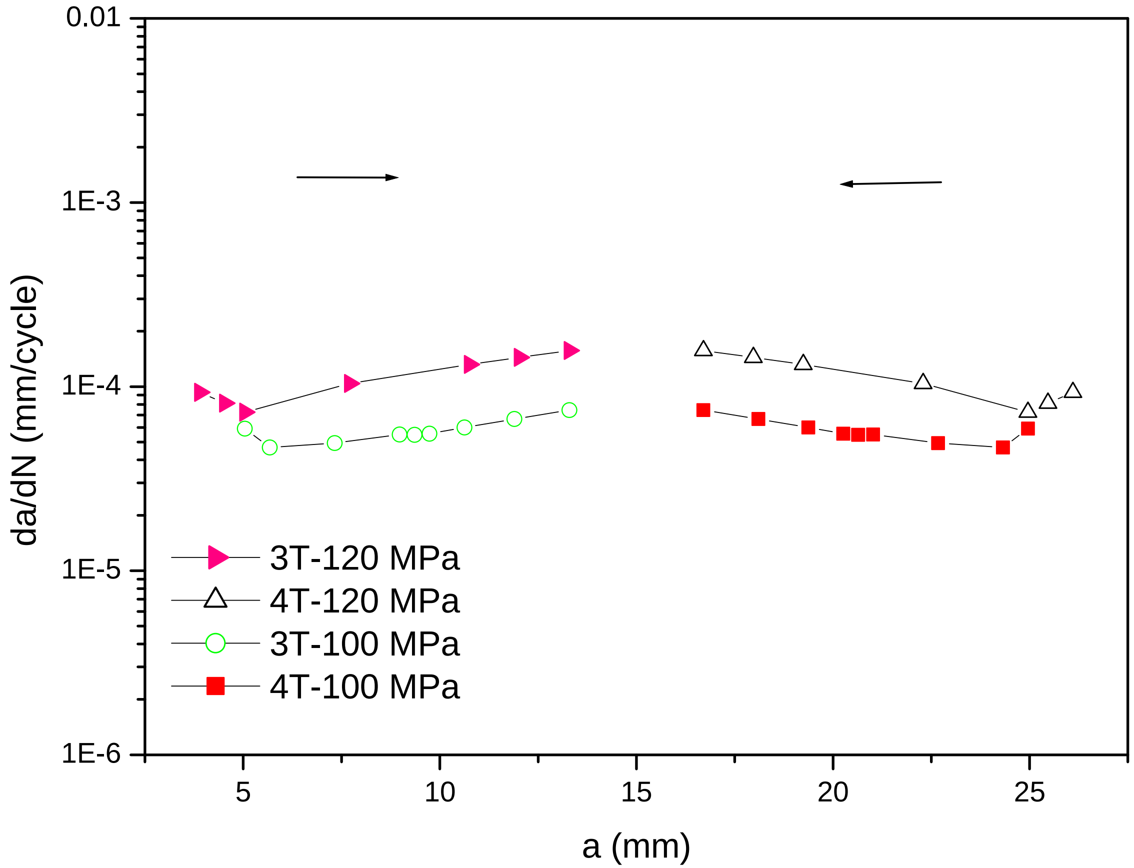

Experiments and prediction

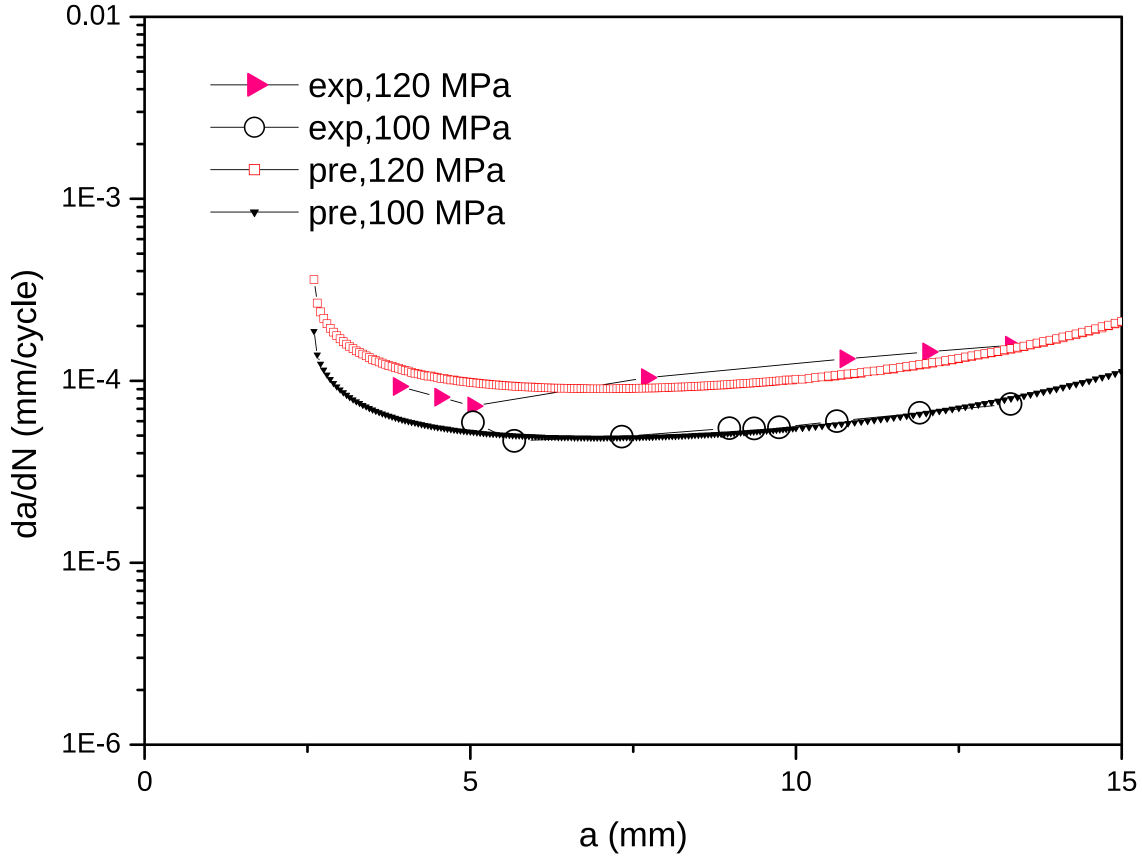

Residual strength in fiber metal laminates with MSD

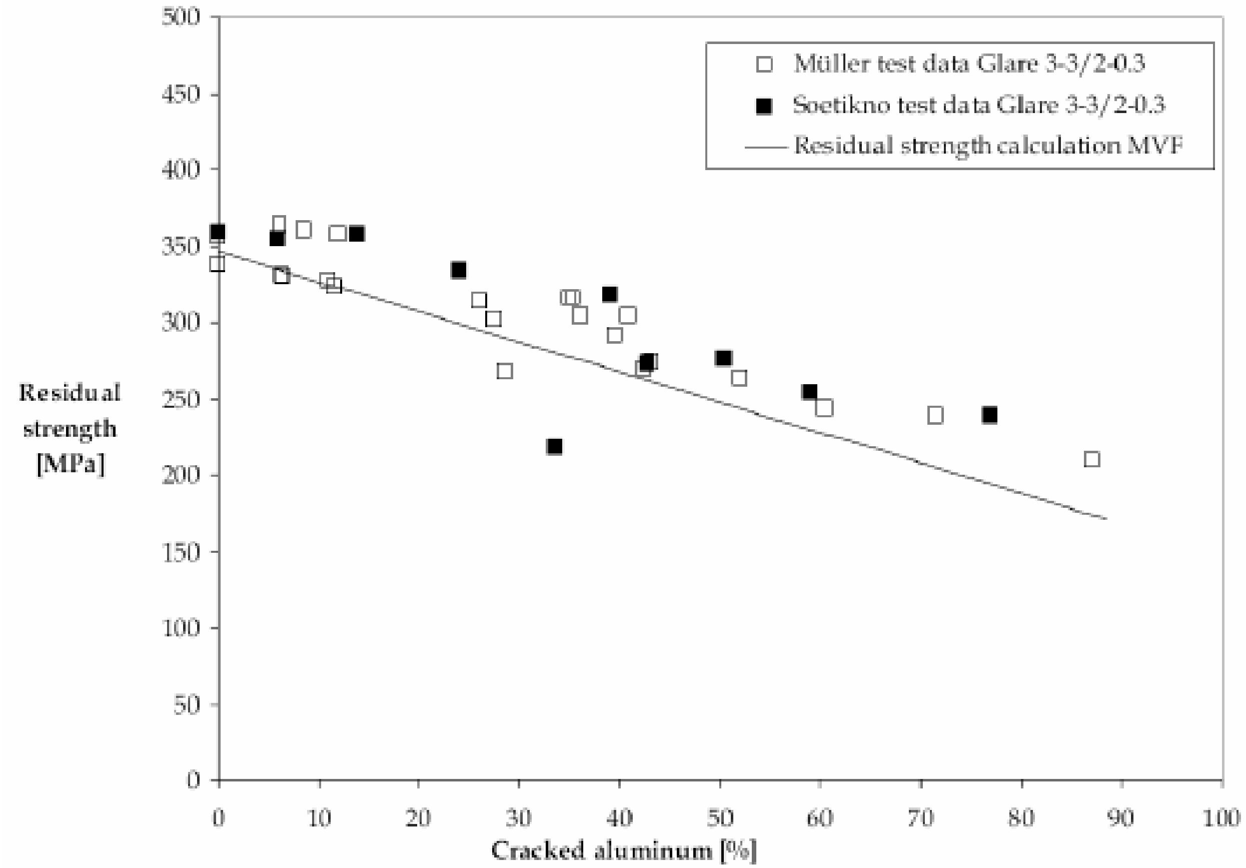

T. Buemler, Flying Glare, 2004

Conclusion

- The crack growth behavior of a fiber metal laminate with multiple site damage has been investigated experimentally and analytically.
- When the fatigue cracks emanated from the open holes and propagated, the crack growth rate was faster with the presence of MSD cracks as compared to the case without the presence of MSD cracks.
- The proposed methodology for predicting the crack growth rates of Glare laminates with multiple-site fatigue damage was validated with experiments

Numerical Simulation for Single & Multiple Impacts

Single Impact – Finite Element Model

- Boundary Conditions:
  - "Perfect clamping" at the circular edge of the specimen
  - Symmetry boundary conditions imposed at the centerline
  - An initial velocity is specified for the impactor, at the moment of impact. Gravitational acceleration is not necessary
- Rigid Impactor
  - Discrete rigid body
  - Initially in contact with a single node of the specimen at time zero
  - Constrained to move only along the line of impact

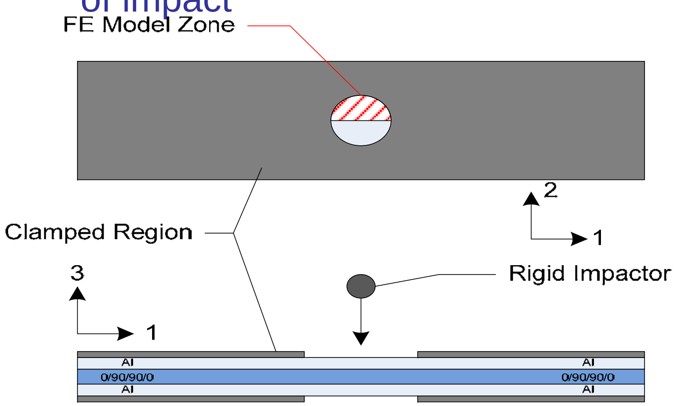

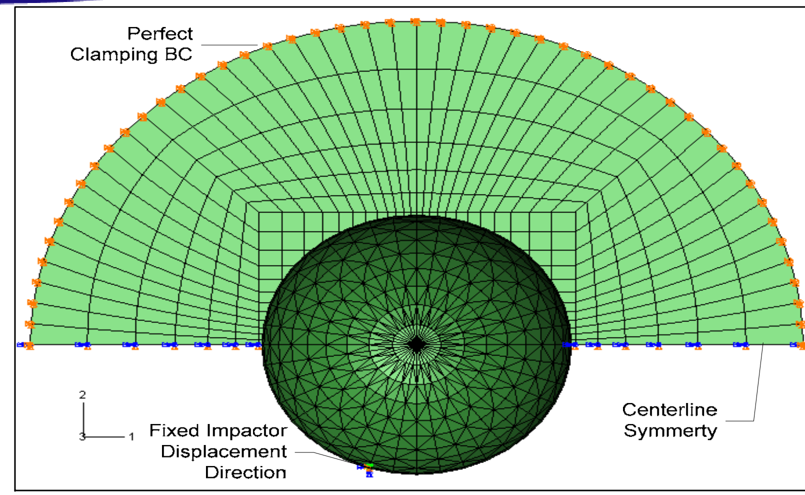

- Model Geometry:
  - GLARE 5-2/1, GLARE 4-3/2
  - Aluminum thickness = 0.489mm
  - Glass-Epoxy thickness = 0.146mm
  - Impact zone diameter of 31.7mm
  - Spherical impactor diameter of 12.7mm
- Data Measurement:
  - Contact force is measured in the direction parallel to impact
  - Transducer measurements are simulated by determining contact force output at all nodes in contact at a given time

2D and 3D failure Criteria

- As a consequence of the planar assumption, required by most commercial finite element programs, non-linear behavior of the material can be significantly underestimated if the out-of-plane components are non-trivial.
- Consider Hashin's 3D composite failure criteria [1]:

Neglected Components

Fiber Tension Failure Mode

$$f_{ft} = \left(\frac{\varepsilon_{11}}{\varepsilon_{11+}^{init}}\right)^2 + \frac{1}{\varepsilon_{12}^{init\ 2}}\left(\varepsilon_{12}^2 + \varepsilon_{13}^2\right) \geq 1$$

Fiber Compression Failure Mode

$$f_{fc} = \frac{-\varepsilon_{11}}{\varepsilon_{11-}^{init}} \geq 1$$

Matrix Tension Failure Mode

$$f_{mt} = \frac{1}{\varepsilon_{22+}^{init\ 2}}\left(\varepsilon_{22} + \varepsilon_{33}\right)^2 + \frac{1}{\varepsilon_{12}^{init\ 2}}\left(\varepsilon_{23}^2 + \varepsilon_{12}^2 + \varepsilon_{13}^2 - \varepsilon_{22}\varepsilon_{33}\right) \geq 1$$

Matrix Compression Failure Mode

$$f_{mc} = \frac{1}{\varepsilon_{22-}^{init}}\left[\left(\frac{\varepsilon_{22-}^{init}}{2\varepsilon_{12}^{init}}\right)^2 - 1\right]\left(\varepsilon_{22} + \varepsilon_{33}\right) + \frac{1}{\varepsilon_{12}^{init\ 2}}\left[\frac{\varepsilon_{22}^2 + \varepsilon_{33}^2}{2} + \varepsilon_{23}^2 + \varepsilon_{12}^2 + \varepsilon_{13}^2\right] \geq 1$$

- Are the through-thickness terms something to be concerned about?

  "[T]hree-dimensional effects are predominant at the edge of the hole and limit the significance of [a planar] approach." – de Jong

- In order to incorporate three-dimensional effects into the fiber metal laminate finite element models, we need to develop our own composite failure subroutines…

Dynamic Progressive Damage Subroutine

- This damage mechanics formulation has been incorporated in a User Material FORTRAN subroutine (VUMAT).
- Specifically, it's used with the ABAQUS Explicit solver, but the methods apply to any commercial finite element code based on explicit integration
- Essentially, the process flow is as follows:

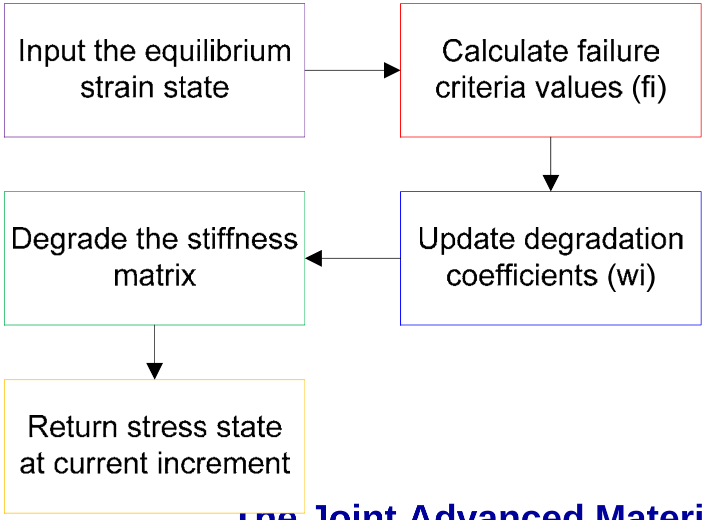

- From the ABAQUS GUI, the user defines a "block" of elements, each of which is assumed to initially have the same material properties

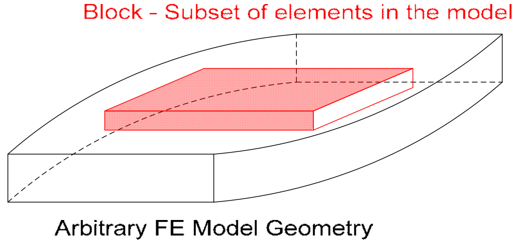

- At the initial time step, the subroutine computes the elastic wave speed, which is used to determine the allowable step time for the analysis

$$\Delta t = \min_{i=1,3}\left(\min_{n=1,nblock}\left[\frac{E_n^L}{v_i^d}\right]\right)$$

Where EL is the characteristic length and vd is the dilational wave speed

- Note that since we have strain softening, the wave speed will decrease with increasing damage. Computing the maximum step time at each increment would improve efficiency

Damage Nucleation and Growth

- Recalling that Hashin's failure criteria predicts four distinct failure modes:
  - Fiber tension (breaking of fibers)
  - Fiber compression (buckling)
  - Matrix tension (cracking of matrix)
  - Matrix compression (crushing)
- It makes sense to have a unique degradation value (wi) for each mode

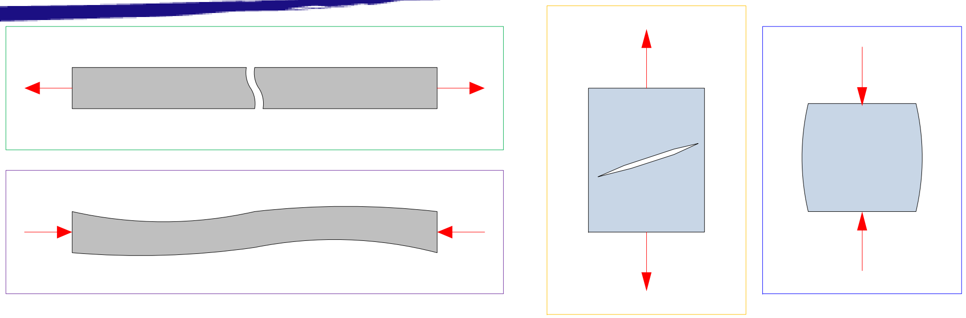

Failure Mode Schematic

- From the damage mechanics assumption [4], rate of degradation is assumed to be composed of a nucleation term (0) and a growth term (1)

$$\dot{w}_i\left(t+\Delta t\right)=\Omega_0+\Omega_1 w_i(t)\left[\left(\frac{\varepsilon\left(t+\Delta t\right)}{\varepsilon^{threshold}}\right)^2-1\right] \quad \textbf{where } \Omega_i \textbf{ are constants}$$

- Where the "threshold" required to produce damage is assumed to decrease with increasing damage density. In other words, cracking is easier if more cracks are present

$$\varepsilon_i^{threshold}=\varepsilon_i^{init}\left(1-w_i\left(t\right)\right)$$

- Since the individual step time is small, we assume a linear form for the degradation rate

$$\dot{w}_i\left(t+\Delta t\right)\approx\frac{w_i\left(t+\Delta t\right)-w_i(t)}{\Delta t}\rightarrow\boxed{w_i\left(t+\Delta t\right)\approx w_i(t)+\dot{w}_i\left(t+\Delta t\right)\Delta t} \quad \textbf{where } \Delta \textbf{t} << \textbf{1}$$

Damage and Constitutive Relations

- Once a failure criteria value exceeds one, it produces a non-zero damage growth rate. The effective element stress is reduced by adjusting the elastic constants

	Degraded Material Properties					
Failure Mode	E11	E22	v12	v23	G12	G23
Fiber Tension	X		X		X	
Fiber Compression	X		X		X	
Matrix Tension		X	X	X	X	X
Matrix Compression		X	X	X	X	X

- Where the amount of damage is linked to the degradation functions as follows:

$$E'_{11} = \left(1 - w_{ft}\right)\left(1 - w_{fc}\right) E_{11}$$

$$v'_{12} = \left(1 - w_{ft}\right)\left(1 - w_{fc}\right)\left(1 - w_{mt}\right)\left(1 - w_{mc}\right) v_{12}$$

- Finally, the compliance matrix is evaluated at each integration point and inverted to get the material stiffness

$$S_D = \begin{bmatrix} 1/E'_{11} & -v'_{12}/E'_{11} & -v'_{12}/E'_{11} & 0 & 0 & 0 \\ -v'_{12}/E'_{11} & 1/E'_{22} & -v'_{23}/E'_{22} & 0 & 0 & 0 \\ -v'_{12}/E'_{11} & -v'_{23}/E'_{22} & 1/E'_{22} & 0 & 0 & 0 \\ 0 & 0 & 0 & 1/G'_{12} & 0 & 0 \\ 0 & 0 & 0 & 0 & 1/G'_{12} & 0 \\ 0 & 0 & 0 & 0 & 0 & 1/G'_{23} \end{bmatrix}$$

Where: $C_D = S_D^{-1}$ and $\sigma(t+\Delta t) = C_D \varepsilon (t+\Delta t)$

Input Parameters for Single Impact

The type of numerical analysis	ABAQUS Explicit
Impact energy (J)	11.4, 12.7, 16.3, 16.8
Impact velocity (msec)	1.9, 2.01, 2.28, 2.31
Element type for aluminum layer	C3D8R (solid element)
Element type for composite layer	SC8R (shell), C3D8R (solid)
Failure criteria for composite layer	Hashin failure criteria (2D and 3D)
Tangential frictional factor	0.1
Hourglass control approach	The pure stiffness
Displacement hourglass scaling factor	0.05, 0.1, 0.15
Rotational hourglass scaling factor	0.05, 0.1, 0.15
Out-of-plane displacement hourglass scaling factor	0.05, 0.1, 0.15

Single Impact of GLARE5-2/1: E=12.7J

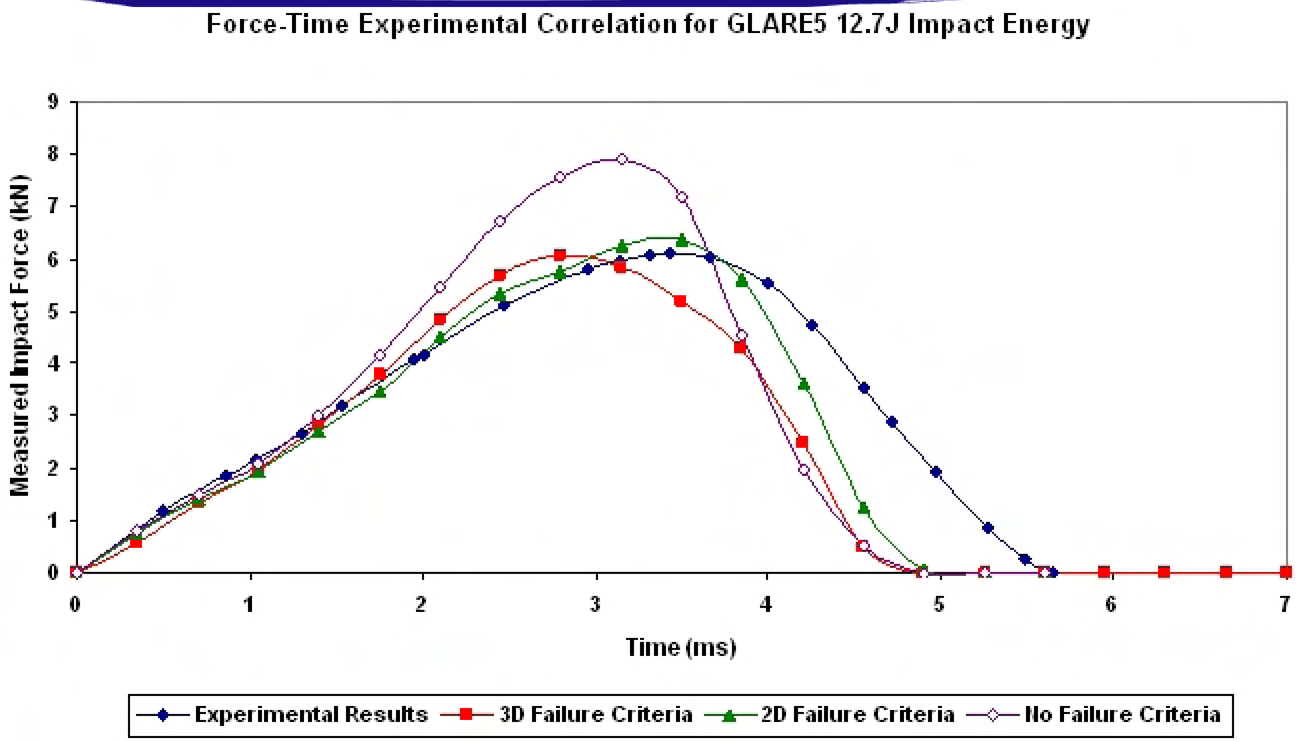

- For low energy impact, it's clear that the three-dimensional failure criteria model is capable of predicting the impact response of the material
- At this energy, there is no significant difference between the two- and three-dimensional criterion. Both represent an improvement over a model which does not incorporate failure
- This represents a limiting case, in which planar failure mechanisms dominate. Damage to the sample is negligible, we call it "Barely Visible Impact Damage (BVID)"

Single Impact of GLARE5-2/1: E=16.3J

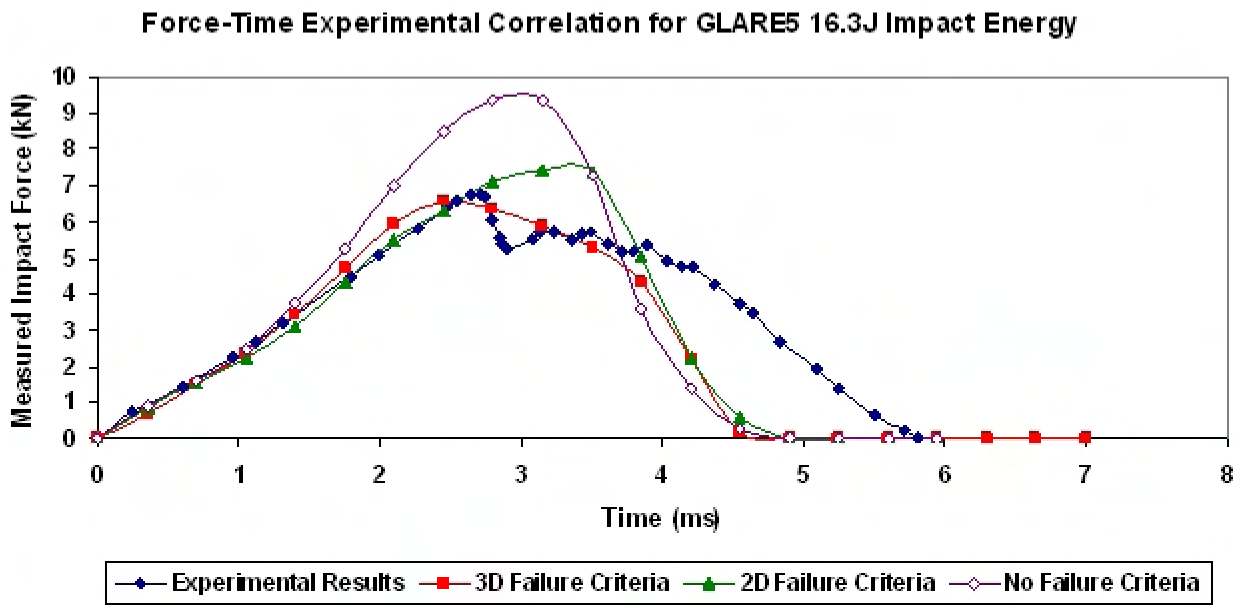

Delamination zone at composite-metal interface

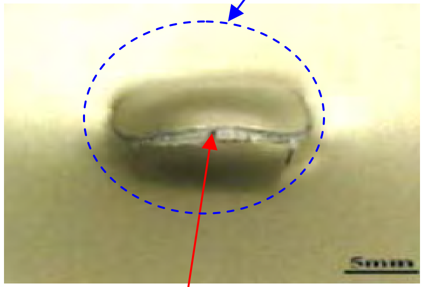

Cracking on the non-impacted side

- At higher impact energies, it is evident that while the correlation is still good, it begins to break down due to damage modes
- Additionally, the impact period is underestimated because of the perfect clamping assumption and one-directional constraint on the rigid impactor.
- As expected, the peak impact force and peak impact time are better predicted using the three-dimensional model. Overall, the three-dimensional model is more conservative than the two-dimensional model

Single Impact of GLARE4-3/2: E=11.4J

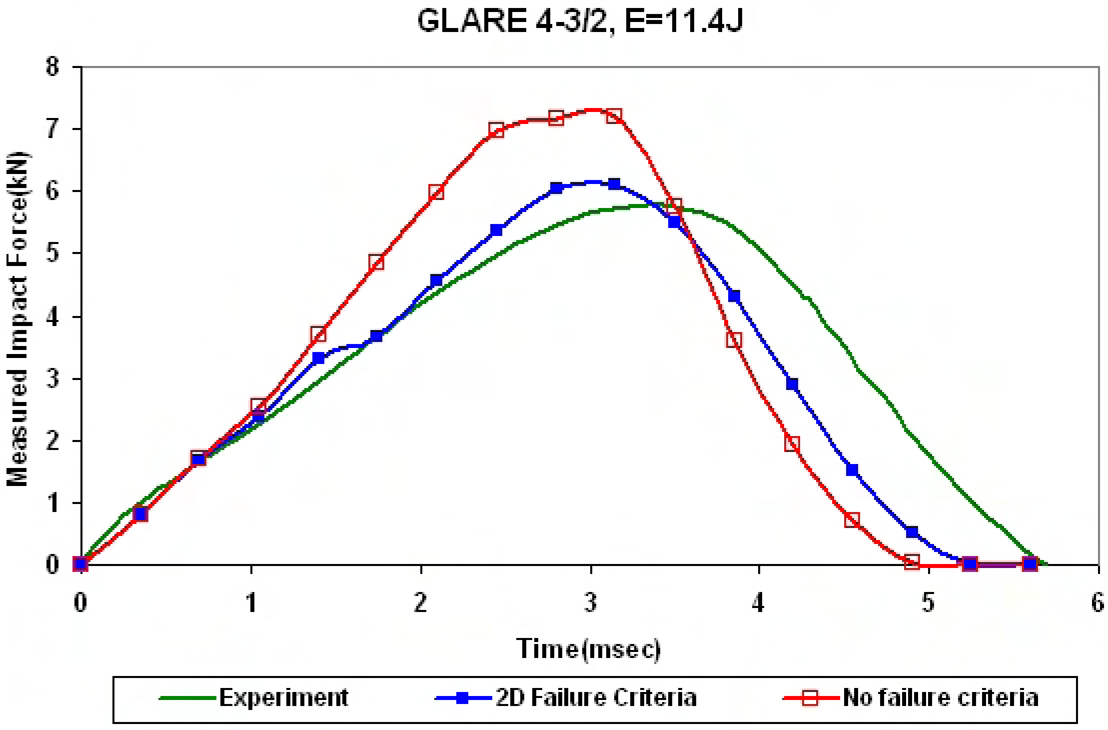

- For low energy impact, it's clear that the two-dimensional failure criteria model is capable of predicting the impact response of the material
- At this energy, as shown in GLARE 5-2/1 there are plastic deformation only
- This represents a limiting case, in which planar failure mechanisms dominate. Damage to the sample is negligible, we call it "Barely Visible Impact Damage (BVID)"

Impact Damage: Composite Damage at GLARE 5-2/1 and GLARE 4-3/2

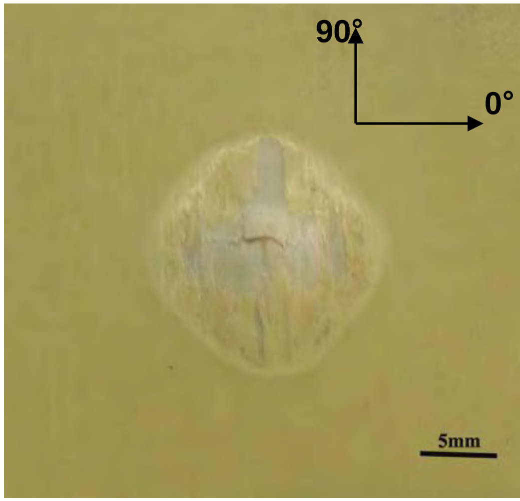

Damage of composite layer at GLARE5-2/1

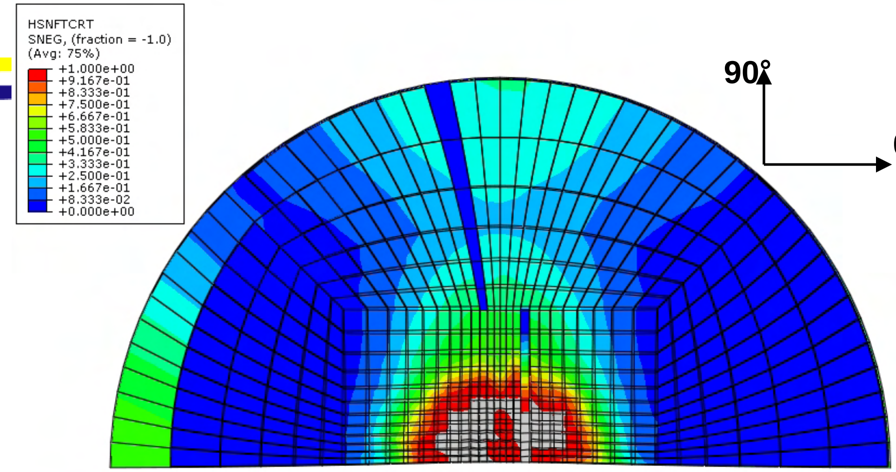

FEM damage of composite layer [0°/90°/90°/0°] at GLARE5-2/1

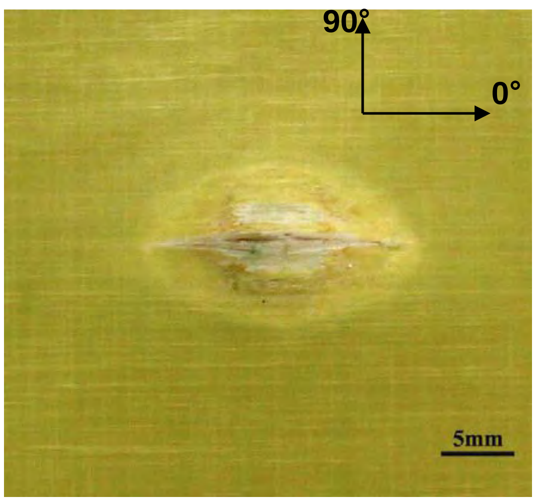

Damage of composite layer at GLARE4-3/2

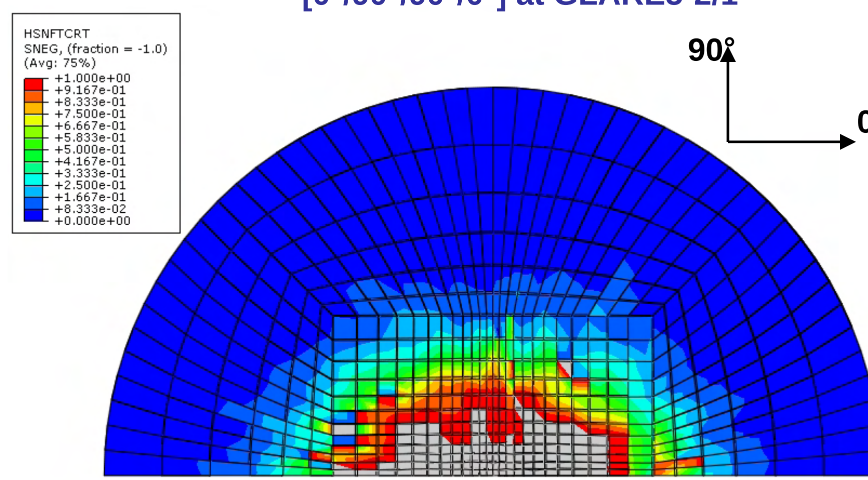

FEM damage of composite layer with [0°/90°/0°] at GLARE4-3/2

Single Impact of GLARE5-2/1 at BVID

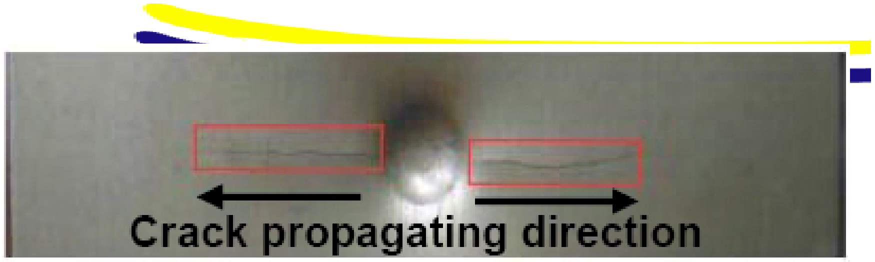

N=115000 cycle

Crack propagation at impacted Al layer

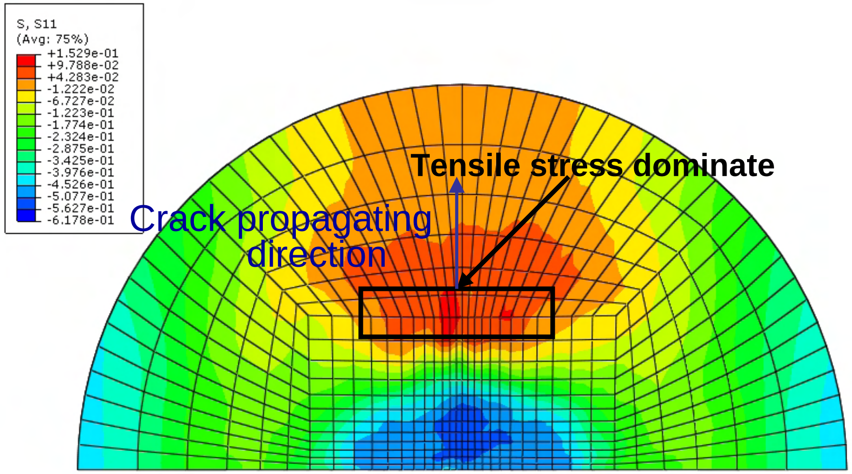

1-directional stress at impacted Al layer

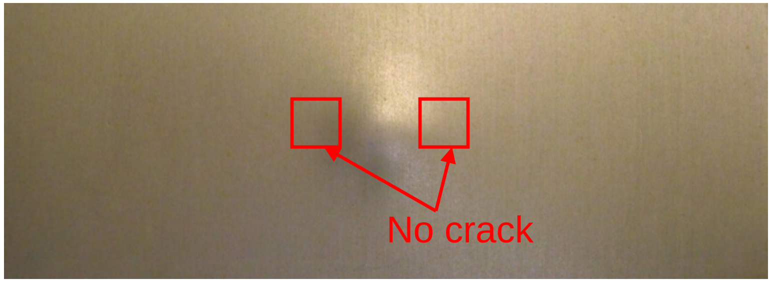

Dent damage at non-impacted Al layer

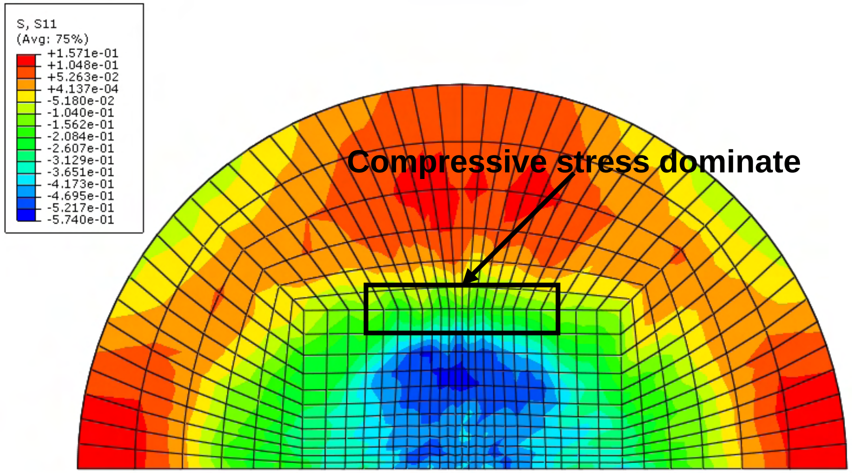

1-directional stress at non-impacted Al layer

When we check 1-directional stress at impacted and non-impacted side for crack initiation, tensile stress dominates impacted Al layer. But at non-impacted Al layer compressive stress dominates. Therefore, when tensile load apply to 1 direction in fatigue behavior, crack initiate on impacted Al layer only.

Single Impact of GLARE4-3/2 at BVID

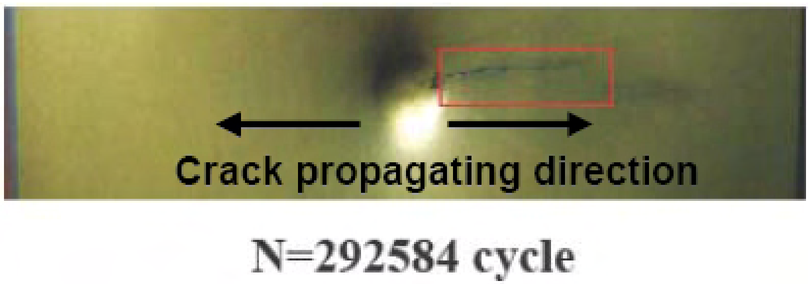

Crack propagation at impacted Al layer

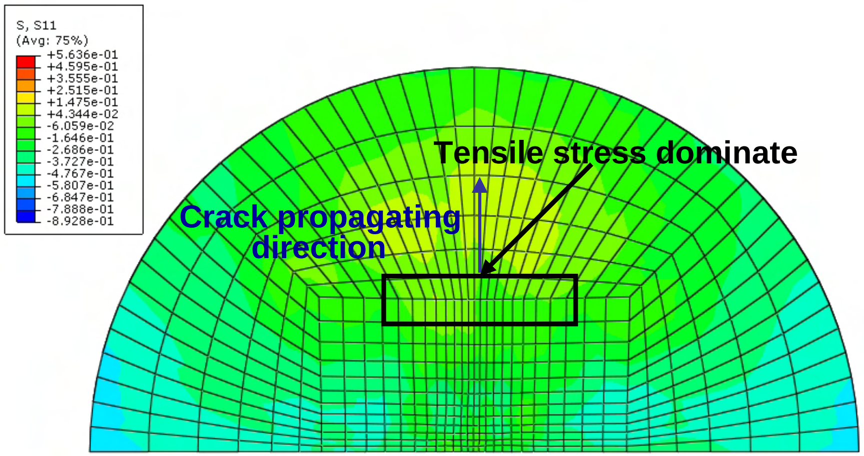

1-directional stress at impacted Al layer

GLARE 4-3/2 also show crack just initiate on impacted Al layer as shown in GLARE 5-2/1.

Investigation of Stress on Aluminum Layer-GLARE5-2/1

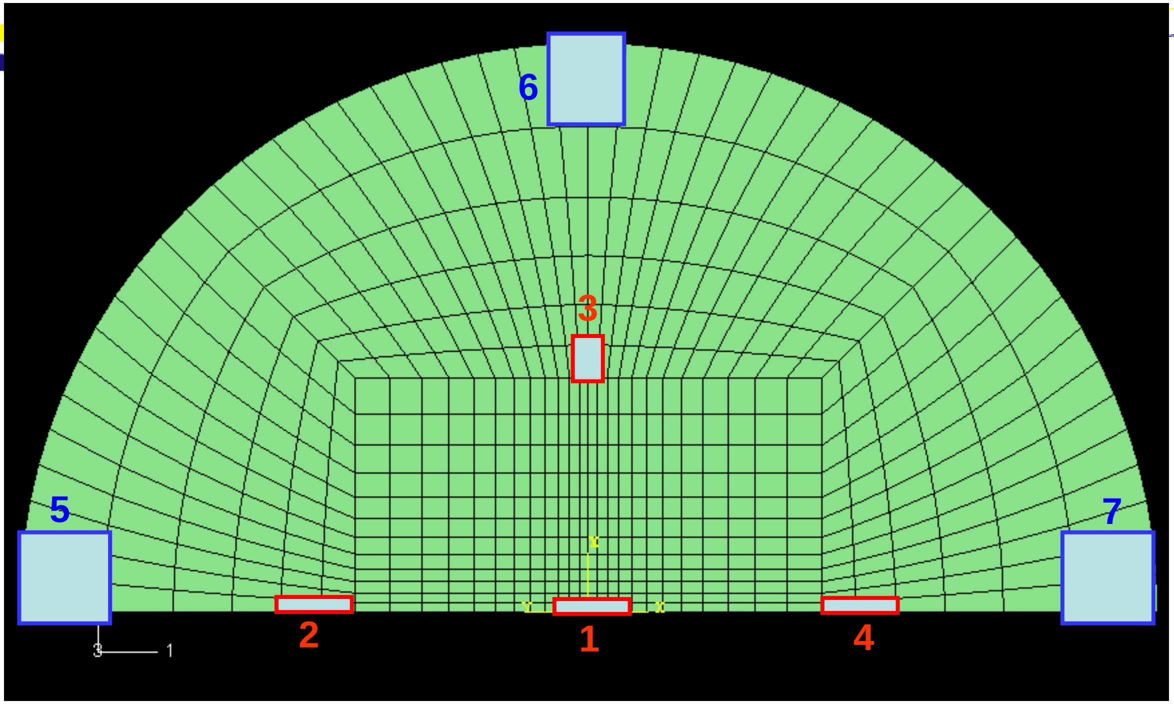

<Von-Misses Stress>

Stress (MPa)	1	2	3	4	5	6	7
12.7J-impacted	435	313	282	312	436	430	446
12.7J-non-impacted	445	306	309	303	241	206	234
16.3J-impacted	408	347	362	374	432	414	441
16.3J-non-impacted	364	298	296	319	234	219	200

Investigation of Stress on Aluminum Layer-GLARE5-2/1

<Stress for 1-direction> - - - - - -> Tensile loading direction

Stress (MPa)	1	2	3	4	5	6	7
12.7J-impacted	-456	-234	81	-216	-389	35	-390
12.7J-non-impacted	-449	-268	-231	-261	-281	-57	-287
16.3J-impacted	-481	-293	72	-294	-410	13	-415
16.3J-non-impacted	-445	-292	-298	-284	-285	-56	-271

Impact dent Crack initiation Nuisance crack

- **Impact dent (1):** By impact force, compressive stress dominate on impacted and non-impacted side of aluminum.
- **The outer impact dent (3)**

 - Impacted side: Since the fiber layers would be elastically deformed and the outer concave dent region experience the state of tension.

 - Non-impacted side: By elastic deformation of fiber layer, the compressive loading occurred on non-impacted aluminum layer.

- **The nuisance crack (5&7)**: To investigate nuisance cracks, stresses were detected on region 5 and 7. Impacted and non-impacted of aluminum layers experience compressive loading. However, these numerical results isn't enough to explain them. Since the nuisance cracks were exhibited randomly under high tensile fatigue loading level. Therefore, it is needed to apply tensile loading to impacted numerical model.

Multiple Impacts – Finite Element Model

- Boundary Conditions:
  - "Perfect clamping" at the circular edge of the specimen
  - Symmetry boundary conditions imposed at the centerline
  - An initial velocity is specified for the impactor, at the moment of impact. Gravitational acceleration is not necessary
- Rigid Impactor
  - Discrete rigid body
  - Initially in contact with a single node of the specimen at time zero
  - Constrained to move only along the line of impact

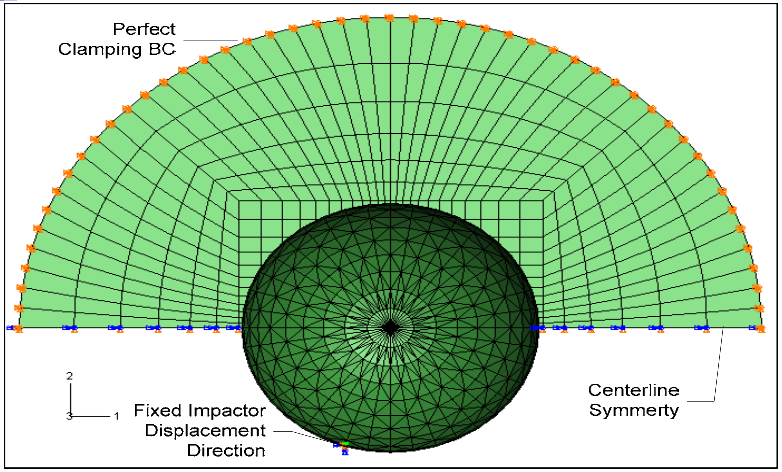

- Model Geometry:
  - GLARE 5-2/1, GLARE 4-3/2
  - Aluminum thickness = 0.489mm
  - Glass-Epoxy thickness = 0.146mm
  - Impact zone diameter of 31.7mm
  - Spherical impactor diameter of 12.7mm
- Impact type:
  - Two impacts were applied on same place
  - Transducer measurements are simulated by determining contact force output at all nodes in contact at a given time

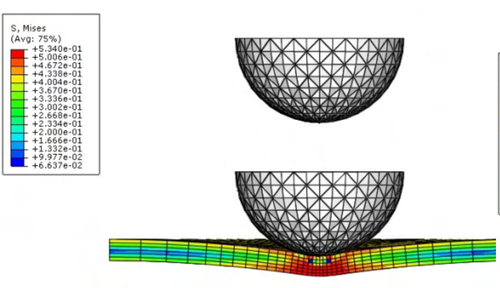

<1st impact>

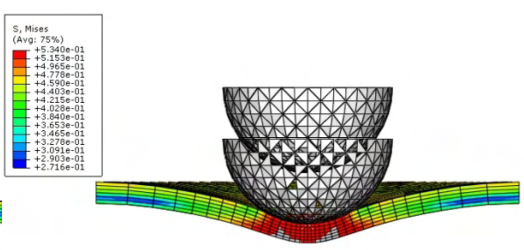

<2nd impact>

Input Parameters for Multiple Impacts

Material name	Aluminum 2024 and GLARE 5-2/1
The type of impact	Multiple impacts at same place
The type of numerical analysis	ABAQUS Explicit
The mesh type	Coarse mesh and fine mesh
Multiple impact energy (J)	8 (4x2) and 16 (8x2)
Impact velocity (msec)	0.797, 1.127, 1.59
Element type for aluminum layer	C3D8R (solid element)
Element type for composite layer	SC8R (shell)
Failure criteria	Hashin failure criteria
Tangential frictional factor	0.1
Hourglass control approach	The pure stiffness
Displacement hourglass scaling factor	0.15
Rotational hourglass scaling factor	0.15
Out-of-plane displacement hourglass scaling factor	0.15

Load-Time: Experiment vs. FEM for AL 2024-T3

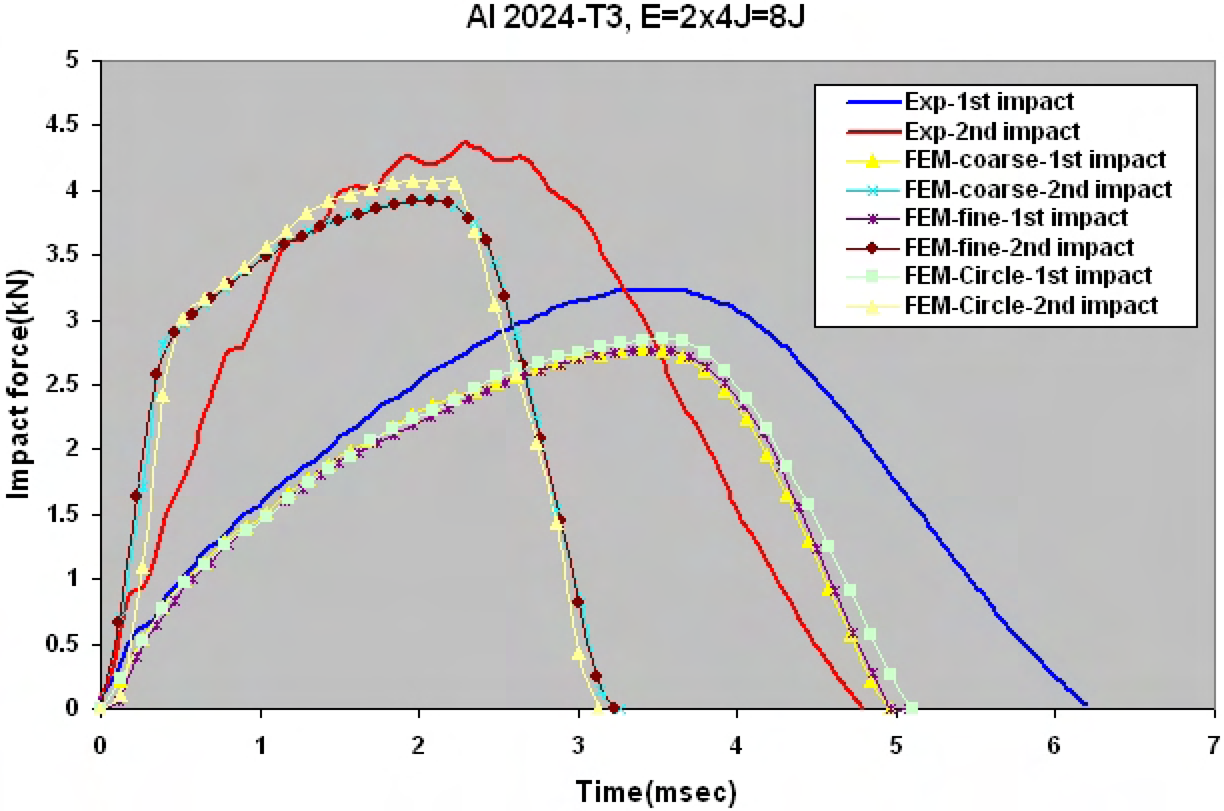

- Multiple Impacts were simulated for diverse mesh type like coarse, fine and circle. As seen in above plot, for impact they aren't different.
- 1st and 2nd impact show plastic deformation and after 2nd impact some vibration was investigated. This vibration may be from stress wave or damping effect. In a simulation, vibration wasn't shown in FEM result.
- Usually, FEM show lower peak impact force than experimental result. This may be caused by full fixed boundary condition.

Load-Time: Experiment vs. FEM for AL 2024-T3 (Cont'd)

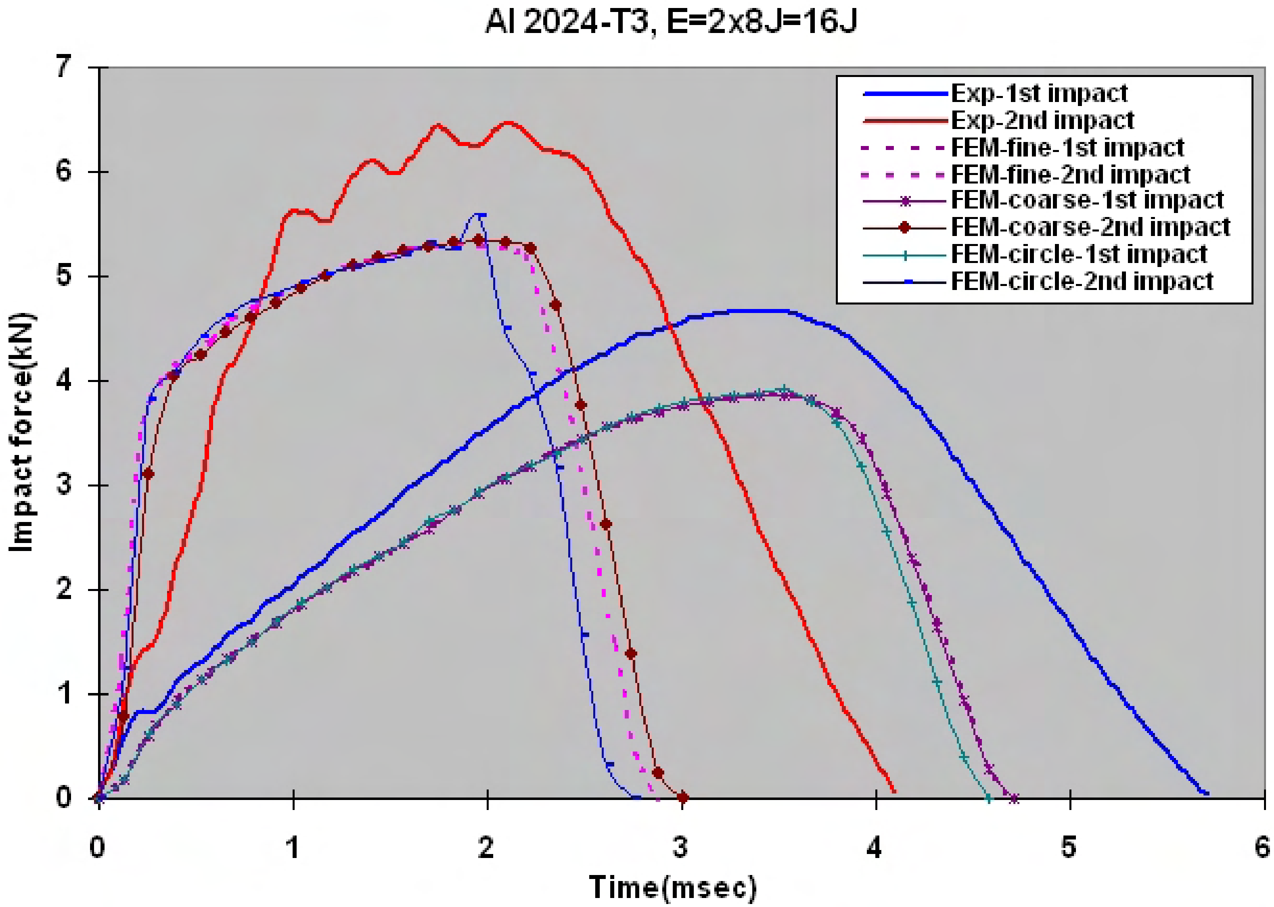

- This FEM result show similar result with impact energy 8J.

Peak Impact Force & Max. Deflection for AL 2024-T3

Comparison of peak impact force (kN)

Impact energy (J)	Experiment (kN)		FEM result (kN)		Error (%)	
	1st	2nd	1st	2nd	1st	2nd
8	3.23	4.36	2.77	3.93	14	9.9
16	4.66	6.47	3.87	5.36	17	17
20	5.31	6.97	4.32	5.77	19	17

Comparison of max. deflection (mm)

Impact energy (J)	Experiment (mm)			FEM result (mm)			Error (%)
	1st	2nd	Total	1st	2nd	Total	
8	2.48	1.76	4.24	2.56	1.46	4.02	5.2
16	3.34	2.12	5.46	3.60	1.90	5.5	0.7
20	3.72	2.47	6.19	4.07	1.97	6.04	2.4

Multiple Impacts for GLARE5-2/1

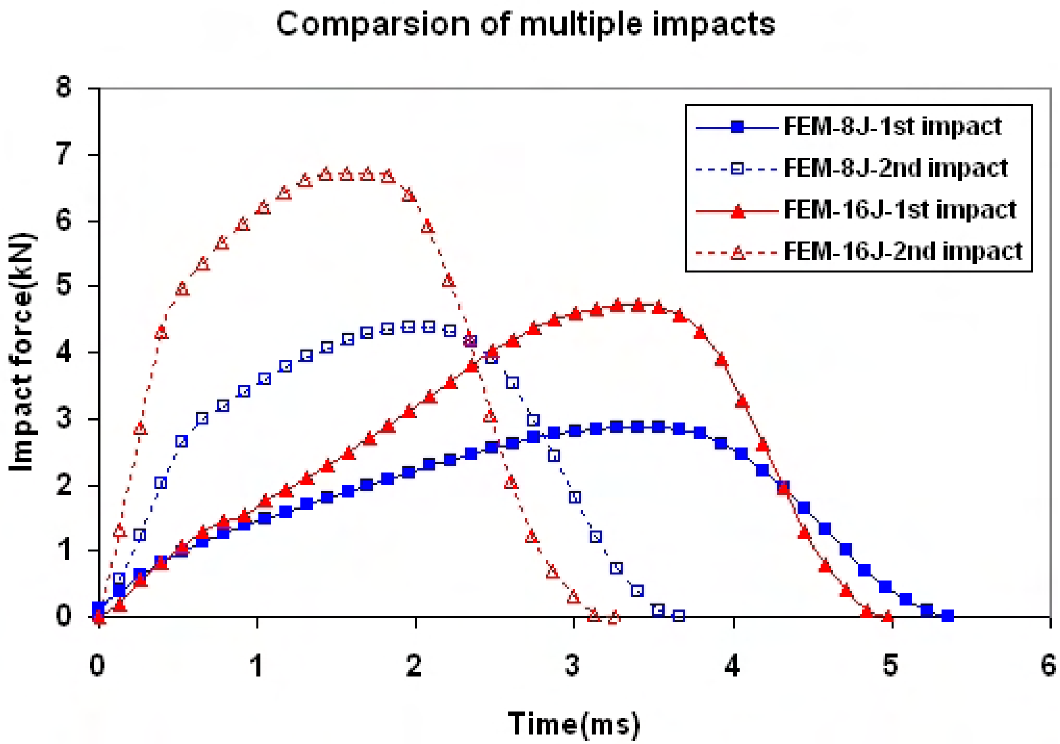

- As increasing impact energy, peak impact force is also increasing.
- Like Al 2024-T3, FEM results for GLARE 5-2/1 show only plastic deformation.
- After 2nd impact, impact force increased sharply. The reason is the degradation rate of stiffness is increasing after 1st impact.

Multiple Impacts Damage for GLARE 5-2/1: E=2x4J=8J

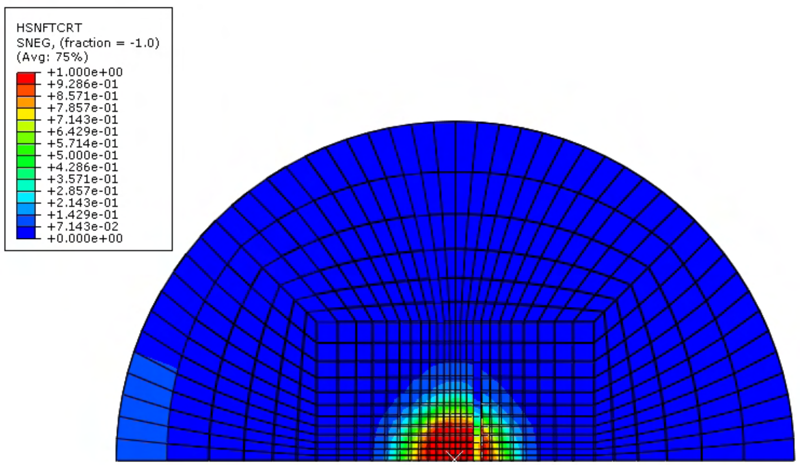

Damage at composite layer after 1st impact

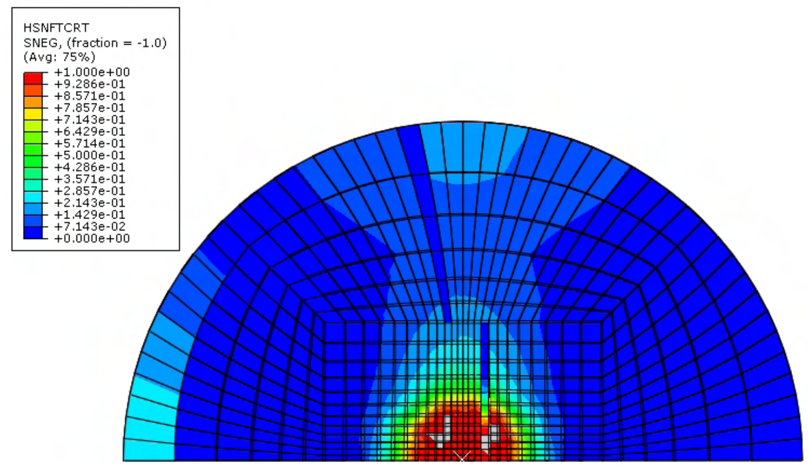

Damage at composite layer after 2nd impact

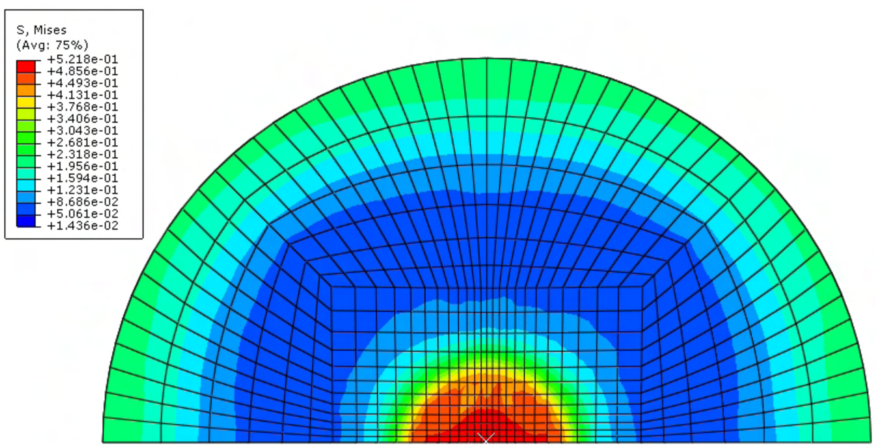

Von-Mises stress at Al layer after 1st impact

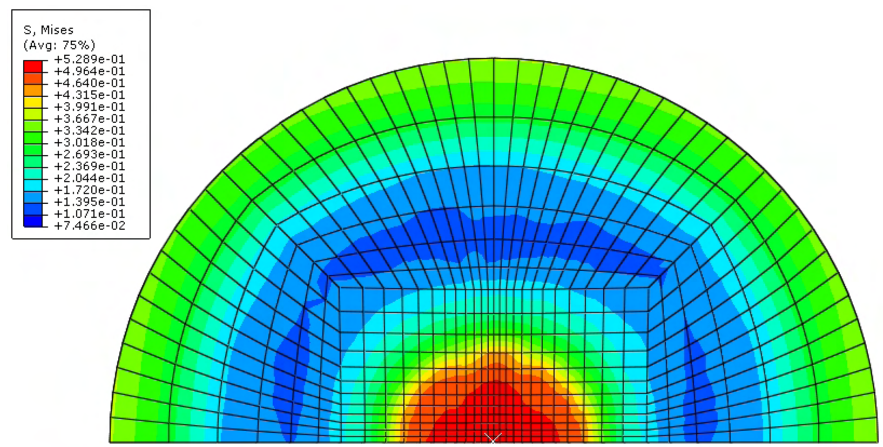

Von-Mises stress at Al layer after 2nd impact

Summary

- Numerical analysis of single impact and multiple impacts for GLARE laminates and aluminum 2024-T3 was conducted. Numerical results for single impact and multiple impacts correlate well with experimental results for impact forces vs. time relationships as well as the stress distribution on aluminum layers on both impacted and non-impacted sides. At the same time, FEM result about maximum deflection showed good agreement compared with experimental results

- In order to predict the occurrence of composite failure and the delamination size, VUMAT (user subroutine to define material behavior) based on 3D failure criterion of numerical analysis was developed. This enabled us to investigate not only failure, the size of delamination of inner composite layers as well as the structural integrity under different impact energies.

- 2D failure criteria was compared with 3D failure criteria depending on different element type. At BVID, there is no significant difference between the 2D and 3D criterion. At CVID, the peak impact force and peak impact time are better predicted using the three-dimensional model. Overall, the three-dimensional model is more conservative than the two-dimensional model. However, both represent an improvement over a model which does not incorporate failure.

A Look Forward

- **Benefit to Aviation**

  --Development of analytical models validated by experiment and the information system are critical to design optimization and to support the airworthiness certification.

- **Future needs**

  --Post-impact fatigue behavior for multiple impacts

  --New generation of fiber metal laminates